Author Contributions

Conceived and designed the experiments: KK KF JY HO YT MN. Performed the experiments: KK KF FT KH. Analyzed the data: KK KF FT KH. Contributed reagents/materials/analysis tools: T. Nomura HF T. Nakamura YT MA HO MN. Wrote the paper: KK HO MN.

References

1. Tuszynski MH, Peterson DA, Ray J, Baird A, Nakahara Y, et al. (1994) Fibroblasts genetically modified to produce nerve growth factor induce robust neuritic ingrowth after grafting to the spinal cord. Exp Neurol 126: 1–14.
2. Tuszynski MH, Gabriel K, Gage FH, Suhr S, Meyer S, et al. (1996) Nerve growth factor delivery by gene transfer induces differential outgrowth of sensory, motor, and noradrenergic neurites after adult spinal cord injury. Exp Neurol 137: 157–173.
3. Jakeman LB, Wei P, Guan Z, Stokes BT (1998) Brain-derived neurotrophic factor stimulates hindlimb stepping and sprouting of cholinergic fibers after spinal cord injury. Exp Neurol 154: 170–184.
4. McTigue DM, Horner PJ, Stokes BT, Gage FH (1998) Neurotrophin-3 and brain-derived neurotrophic factor induce oligodendrocyte proliferation and myelination of regenerating axons in the contused adult rat spinal cord. J Neurosci 18: 5354–5365.
5. Grill R, Murai K, Blesch A, Gage FH, Tuszynski MH (1997) Cellular delivery of neurotrophin-3 promotes corticospinal axonal growth and partial functional recovery after spinal cord injury. J Neurosci 17: 5560–5572.
6. Blesch A, Tuszynski MH (2001) GDNF gene delivery to injured adult CNS motor neurons promotes axonal growth, expression of the trophic neuropeptide CGRP, and cellular protection. J Comp Neurol 436: 399–410.
7. Liu LJ, Zhu JK, Xiao JD (1999) [Rescue of motoneuron from brachial plexus nerve root avulsion induced cell death by Schwann cell derived neurotrophic factor]. Zhongguo Xiu Fu Chong Jian Wai Ke Za Zhi 13: 295–298.
8. Casella GT, Marcillo A, Bunge MB, Wood PM (2002) New vascular tissue rapidly replaces neural parenchyma and vessels destroyed by a contusion injury to the rat spinal cord. Exp Neurol 173: 63–76.
9. Loy DN, Crawford CH, Darnall JB, Burke DA, Onifer SM, et al. (2002) Temporal progression of angiogenesis and basal lamina deposition after contusive spinal cord injury in the adult rat. J Comp Neurol 445: 308–324.
10. Mautes AE, Weinzierl MR, Donovan F, Noble LJ (2000) Vascular events after spinal cord injury: contribution to secondary pathogenesis. Phys Ther 80: 673–687.
11. Guizar-Sahagun G, Ibarra A, Espitia A, Martinez A, Madrazo I, et al. (2005) Glutathione monoethyl ester improves functional recovery, enhances neuron survival, and stabilizes spinal cord blood flow after spinal cord injury in rats. Neuroscience 130: 639–649.
12. Glaser J, Gonzalez R, Perreau VM, Cotman CW, Keirstead HS (2004) Neutralization of the chemokine CXCL10 enhances tissue sparing and angiogenesis following spinal cord injury. J Neurosci Res 77: 701–708.
13. Nakamura T, Nawa K, Ichihara A (1984) Partial purification and characterization of hepatocyte growth factor from serum of hepatectomized rats. Biochem Biophys Res Commun 122: 1450–1459.
14. Nakamura T, Nishizawa T, Hagiya M, Seki T, Shimonishi M, et al. (1989) Molecular cloning and expression of human hepatocyte growth factor. Nature 342: 440–443.
15. Bottaro DP, Rubin JS, Faletto DL, Chan AM, Kmiecik TE, et al. (1991) Identification of the hepatocyte growth factor receptor as the c-met proto-oncogene product. Science 251: 802–804.
16. Caton A, Hacker A, Naeem A, Livet J, Maina F, et al. (2000) The branchial arches and HGF are growth-promoting and chemoattractant for cranial motor axons. Development 127: 1751–1766.
17. Maina F, Klein R (1999) Hepatocyte growth factor, a versatile signal for developing neurons. Nat Neurosci 2: 213–217.
18. Hamanoue M, Takemoto N, Matsumoto K, Nakamura T, Nakajima K, et al. (1996) Neurotrophic effect of hepatocyte growth factor on central nervous system neurons in vitro. J Neurosci Res 43: 554–564.
19. Honda S, Kagoshima M, Wanaka A, Tohyama M, Matsumoto K, et al. (1995) Localization and functional coupling of HGF and c-Met/HGF receptor in rat brain: implication as neurotrophic factor. Brain Res Mol Brain Res 32: 197–210.
20. Funakoshi H NT (2011) Hepatocyte growth factor (HGF): neurotrophic functions and therapeutic implications for neuronal injury/diseases. Current Signal Transduction Therapy 6: 156–67.
21. Date I, Takagi N, Takagi K, Kago T, Matsumoto K, et al. (2004) Hepatocyte growth factor improved learning and memory dysfunction of microsphere-embolized rats. J Neurosci Res 78: 442–453.
22. Miyazawa T, Matsumoto K, Ohmichi H, Katoh H, Yamashima T, et al. (1998) Protection of hippocampal neurons from ischemia-induced delayed neuronal death by hepatocyte growth factor: a novel neurotrophic factor. J Cereb Blood Flow Metab 18: 345–348.
23. Shimamura M, Sato N, Waguri S, Uchiyama Y, Hayashi T, et al. (2006) Gene transfer of hepatocyte growth factor gene improves learning and memory in the chronic stage of cerebral infarction. Hypertension 47: 742–751.
24. Ishigaki A, Aoki M, Nagai M, Warita H, Kato S, et al. (2007) Intrathecal delivery of hepatocyte growth factor from amyotrophic lateral sclerosis onset suppresses disease progression in rat amyotrophic lateral sclerosis model. J Neuropathol Exp Neurol 66: 1037–1044.
25. Kitamura K, Iwanami A, Nakamura M, Yamane J, Watanabe K, et al. (2007) Hepatocyte growth factor promotes endogenous repair and functional recovery after spinal cord injury. J Neurosci Res 85: 2332–2342.
26. Basso DM, Beattie MS, Bresnahan JC (1995) A sensitive and reliable locomotor rating scale for open field testing in rats. J Neurotrauma 12: 1–21.
27. Nowak DD, Lee JK, Gelb DE, Poelstra KA, Ludwig SC (2009) Central cord syndrome. J Am Acad Orthop Surg 17: 756–765.
28. Iwanami A, Yamane J, Katoh H, Nakamura M, Momoshima S, et al. (2005) Establishment of graded spinal cord injury model in a nonhuman primate: the common marmoset. J Neurosci Res 80: 172–181.
29. Terashima T, Ochiishi T, Yamauchi T (1994) Immunohistochemical detection of calcium/calmodulin-dependent protein kinase II in the spinal cord of the rat and monkey with special reference to the corticospinal tract. J Comp Neurol 340: 469–479.
30. Fujiyoshi K, Yamada M, Nakamura M, Yamane J, Katoh H, et al. (2007) In vivo tracing of neural tracts in the intact and injured spinal cord of marmosets by diffusion tensor tractography. J Neurosci 27: 11991–11998.
31. Yamane J, Nakamura M, Iwanami A, Sakaguchi M, Katoh H, et al. (1394-1405)
32. Courtine G, Bunge MB, Fawcett JW, Grossman RG, Kaas JH, et al. (2007) Can experiments in nonhuman primates expedite the translation of treatments for spinal cord injury in humans? Nat Med 13: 561–566.
33. Iwanami A, Kaneko S, Nakamura M, Kanemura Y, Mori H, et al. (2005) Transplantation of human neural stem cells for spinal cord injury in primates. J Neurosci Res 80: 182–190.
34. Jackson AB, Dijkers M, Devivo MJ, Poczatek RB (2004) A demographic profile of new traumatic spinal cord injuries: change and stability over 30 years. Arch Phys Med Rehabil 85: 1740–1748.
35. Phillips CG, Porter R (1977) Corticospinal neurones. Their role in movement. Monogr Physiol Soc: v-xii, 1-450.
36. Shapovalov AI (1975) Neuronal organization and synaptic mechanisms of supraspinal motor control in vertebrates. Rev Physiol Biochem Pharmacol 72: 1–54.
37. Rouiller EM, Moret V, Tanne J, Boussaoud D (1996) Evidence for direct connections between the hand region of the supplementary motor area and cervical motoneurons in the macaque monkey. Eur J Neurosci 8: 1055–1059.
38. Lemon RN, Kirkwood PA, Maier MA, Nakajima K, Nathan P (2004) Direct and indirect pathways for corticospinal control of upper limb motoneurons in the primate. Prog Brain Res 143: 263–279.
39. Heffner R, Masterton B (1975) Variation in form of the pyramidal tract and its relationship to digital dexterity. Brain Behav Evol 12: 161–200.
40. Heffner RS, Masterton RB (1983) The role of the corticospinal tract in the evolution of human digital dexterity. Brain Behav Evol 23: 165–183.
41. Palmer E, Ashby P (1992) Evidence that a long latency stretch reflex in humans is transcortical. J Physiol 449: 429–440.
42. Bernhard CG, Bohm E, Petersen I (1953) New investigations on the pyramidal system in Macaca mulatta. Experientia 9: 111–112.
43. Lemon RN (2008) Descending pathways in motor control. Annu Rev Neurosci 31: 195–218.
44. Sasaki S, Isa T, Pettersson LG, Alstermark B, Naito K, et al. (2004) Dexterous finger movements in primate without monosynaptic corticomotoneuronal excitation. J Neurophysiol 92: 3142–3147.
45. Freund P, Schmidlin E, Wannier T, Bloch J, Mir A, et al. (2006) Nogo-A-specific antibody treatment enhances sprouting and functional recovery after cervical lesion in adult primates. Nat Med 12: 790–792.
46. Nishimura Y, Onoe H, Morichika Y, Perfiliev S, Tsukada H, et al. (2007) Time-dependent central compensatory mechanisms of finger dexterity after spinal cord injury. Science 318: 1150–1155.
47. Nishimura Y, Morichika Y, Isa T (2009) A subcortical oscillatory network contributes to recovery of hand dexterity after spinal cord injury. Brain 132: 709–721.
48. Mansfield K, Tardif S, Eichler E (2004) White Paper for Complete Sequencing of the Common Marmoset (*Callithrix jacchus*) Genome. Available: http://www.genome.gov/Pages/Research/Sequencing/SeqProposals/MarmosetSeq.pdf Accessed 2011 Oct 31.
49. Gelfan S (1964) Neuronal Interdependence. Prog Brain Res 11: 238–260.
50. Bortoff GA, Strick PL (1993) Corticospinal terminations in two new-world primates: further evidence that corticomotoneuronal connections provide part of the neural substrate for manual dexterity. J Neurosci 13: 5105–5118.
51. Ralston DD, Ralston HJ, 3rd (1985) The terminations of corticospinal tract axons in the macaque monkey. J Comp Neurol 242: 325–337.
52. Alstermark B, Isa T, Ohki Y, Saito Y (1999) Disynaptic pyramidal excitation in forelimb motoneurons mediated via C(3)-C(4) propriospinal neurons in the Macaca fuscata. J Neurophysiol 82: 3580–3585.

OPEN ACCESS Freely available online

PLoS one

Schwann-Spheres Derived from Injured Peripheral Nerves in Adult Mice - Their *In Vitro* Characterization and Therapeutic Potential

Takehiko Takagi[1,2], Ken Ishii[1], Shinsuke Shibata[2], Akimasa Yasuda[1,2], Momoka Sato[1,2,3], Narihito Nagoshi[4], Harukazu Saito[4], Hirotaka J. Okano[2], Yoshiaki Toyama[1], Hideyuki Okano[2]*, Masaya Nakamura[1]*

1 Department of Orthopaedic Surgery, Keio University School of Medicine, Tokyo, Japan, **2** Department of Physiology, Keio University School of Medicine, Tokyo, Japan, **3** Center for Integrated Medical Research, Keio University, Tokyo, Japan, **4** Department of Orthopaedic Surgery, Murayama Medical Center, National Hospital Organization, Tokyo, Japan

Abstract

Multipotent somatic stem cells have been identified in various adult tissues. However, the stem/progenitor cells of the peripheral nerves have been isolated only from fetal tissues. Here, we isolated Schwann-cell precursors/immature Schwann cells from the injured peripheral nerves of adult mice using a floating culture technique that we call "Schwann-spheres." The Schwann-spheres were derived from de-differentiated mature Schwann cells harvested 24 hours to 6 weeks after peripheral nerve injury. They had extensive self-renewal and differentiation capabilities. They strongly expressed the immature-Schwann-cell marker p75, and differentiated only into the Schwann-cell lineage. The spheres showed enhanced myelin formation and neurite growth compared to mature Schwann cells *in vitro*. Mature Schwann cells have been considered a promising candidate for cell-transplantation therapies to repair the damaged nervous system, whereas these "Schwann-spheres" would provide a more potential autologous cell source for such transplantation.

Citation: Takagi T, Ishii K, Shibata S, Yasuda A, Sato M, et al. (2011) Schwann-Spheres Derived from Injured Peripheral Nerves in Adult Mice - Their *In Vitro* Characterization and Therapeutic Potential. PLoS ONE 6(6): e21497. doi:10.1371/journal.pone.0021497

Editor: Thierry Amédée, Centre National de la Recherche Scientifique, University of Bordeaux, France

Received March 14, 2011; **Accepted** May 30, 2011; **Published** June 24, 2011

Funding: This work was supported by grants from the Leading Project for Realization of Regenerative Medicine from the Ministry of Education, Culture, Sports, Science and Technology (MEXT), Japan, from the Japan Science and Technology Corporation (JST), and from the General Insurance Association of Japan. This work was also supported by a Keio University grant-in-aid for the encouragement of young medical scientists, by grants-in-aid for scientific research from MEXT, Japan, by a grant-in-aid for research fellowship for young scientists from the Japan Society for the Promotion of Science, and by a grant-in-aid from the Global COE Program of MEXT, Japan to Keio University. The funders had no role in study design, data collection and analysis, decision to publish, or preparation of the manuscript.

Competing Interests: This work was supported by grants from the General Insurance Association of Japan. This does not alter the authors' adherence to all the PLoS ONE policies on sharing data and materials.

* E-mail: masa@sc.itc.keio.ac.jp (MN); hidokano@sc.itc.keio.ac.jp (HO)

Introduction

In recent years, multipotent somatic stem cells have been identified in various adult tissues. In the peripheral nerves, stem/progenitor cells that are self-renewing and multipotent, with the potential to differentiate into neurons, glial cells, and myofibroblast, have been detected and isolated from fetal [1], but not adult tissues.

After peripheral nerve injury, mature Schwann cells undergo a reversion in their molecular phenotype, and come to resemble those observed in fetal immature nerves [2]. However, no report has explored how far these cells dedifferentiate, even though recent progress in understanding neural-crest and Schwann-cell development has revealed a rather complete picture of glial development in the early peripheral nerves [3]. In the present study, we sought to determine whether mature Schwann cells in adult peripheral nerves that dedifferentiate into stem/progenitor cells after injury could form spheres in floating culture conditions, even though such spheres cannot be obtained by culturing the dissociated cells of intact peripheral nerves from neonates [4] or adult mice [5].

Here, we cultured the dedifferentiated Schwann cells obtained from the injured peripheral nerves of adult mice at the specific time-point under the floating culture condition and isolated Schwann-cell precursors/immature Schwann cells, as spheres, which we called "Schwann-spheres." This is the first report showing that "Schwann-spheres" can be obtained from adult peripheral nerves. Moreover, their differentiation, myelination, and neurite growth promoting properties *in vitro* suggested their potential use in cell transplantation therapy for the damaged nervous system.

Materials and Methods

Animals and surgical procedures

Normal, specific pathogen-free, adult C57BL/6J mice were purchased from CLEA Japan, Inc., Tokyo, Japan. Nestin-EGFP transgenic mice carry enhanced green fluorescent protein (EGFP) under the control of the second intronic enhancer of the nestin gene, which acts selectively in stem/progenitor cells [6]. Transgenic mice expressing Cre recombinase under control of the MBP promoter (MBP-Cre)[7] were mated with EGFP reporter

mice (CAG-CAT$^{loxP/loxP}$-EGFP) [8] to obtain MBP-Cre/Floxed-CAG-EGFP double-transgenic mice [9].

The adult C57BL/6J mice, Nestin-EGFP mice, and MBP-Cre/Floxed-CAG-EGFP mice (female, 7-8 weeks old) were anesthetized using an intraperitoneal injection of ketamine (100 mg/kg) and xylazine (10 mg/kg). The animals were housed in groups under a 12-hour light/dark cycle, with access to food and water ad libitum. The sciatic nerve was exposed through a dorsal gluteal muscle-splitting approach. The nerve was subjected to a contusive injury at the sciatic notch using a brain aneurysm clip (Sugita clip; Mizuho Ikakogyo, Tokyo, Japan). The clip was closed and left in place for 5 min with a holding force of approximately 50 g. All interventions and animal care procedures were performed in accordance with the Laboratory Animal Welfare Act, the Guide for the Care and Use of Laboratory Animals (National Institutes of Health), and the Guidelines and Policies for Animal Surgery provided by the Animal Study Committee of Keio University, and were approved by the Ethics Committee of Keio University.

Sphere-forming cultures

Cells were dissociated from the distal portion of sciatic nerves before the injury and at 6 or 24 hours, 3, 7, or 10 days, or 2, 3, or 6 weeks after the injury. The cells (1×10^5 cells/ml) were transferred to a sphere-forming floating medium consisting of DMEM/F-12 (1:1) (Gibco, Carlsbad, CA, USA) supplemented with insulin (25 mg/ml), transferrin (100 mg/ml), progesterone (20 nM), sodium selenate (30 nM), putrescine (60 nM) (all from Sigma-Aldrich, St. Louis, USA), recombinant human EGF (100 ng/ml) (Pepro Tech, Rocky Hill, NJ, USA), human FGF-basic (100 ng/ml) (Pepro Tech), B27 (20 ng/ml) (modified from Nagoshi et al. [10]), and 10% FBS (Equitech-Bio, Kerrville, TX, USA). By comparison, neural crest stem cells (NCSCs) were dissociated from the E14.5 dorsal root ganglion (DRG) and neural stem cells (NSCs) were dissociated from the E14.5 striatum [11]. The NCSCs and NSCs were transferred to the sphere-forming floating medium without FBS. The cells were cultured in an incubator at 37°C for 7 days. For clonal sphere expansion, the cells were cultured in the above medium with 0.8% methylcellulose (Nacalai Tesque, Kyoto, Japan) [12].

For the secondary sphere formation assays, the 7-day primary spheres were collected, incubated in 0.25% trypsin-EDTA for 30 min at 37°C, and triturated until a single-cell suspension was obtained. The cells were centrifuged at 800 rpm for 5 min at 4°C, and resuspended in the aforementioned sphere culture medium. The NCSCs and NSCs were resusupended in the sphere culture medium without FBS.

Characterization of spheres derived from injured peripheral nerves

Assays using nestin-EGFP and MBP-Cre/Floxed-EGFP mice. Spheres obtained from the contused sciatic nerves of 7-8-week-old adult Nestin-EGFP mice and MBP-Cre/Floxed-EGFP mice were verified by direct EGFP-fluorescent imaging to be Nestin-positive and derived from MBP-positive cells.

Immunocytochemistry. Spheres were postfixed for 6 hours in 4% paraformaldehyde (PFA), soaked overnight in 10% sucrose followed by 30% sucrose, and embedded in cryomolds for sectioning at 6–8 μm. The spheres were immunostained using the anti-undifferentiated-cell marker, Nestin (mouse IgG1, 1:200, BD Pharmingen, San Jose, CA); Schwann-cell markers, P0 (PZO; chick IgG, 1:200, Aves Labs, Tigard, OR, USA) and p75 (rabbit IgG, 1:200, Chemicon, Billerica, MA, USA), or the proliferative-cell marker, PCNA (rabbit IgG, 1:500, Oncogene Research Product, La Jolla, CA, USA), to define the cell population. Immunoreactivity was visualized using secondary antibodies conjugated with Alexa 488 or Alexa 555 (Molecular Probes). Nuclear counterstaining was performed with Hoechst 33342 (10 mg/ml, Sigma, St. Louis, MO, USA). The samples were observed with a universal fluorescence microscope (AxioImager M1; Carl Zeiss, Jena, Germany).

Differentiation analysis. Spheres were plated on poly-L-lysine (PLL) (Sigma)-coated 8-well chamber slides (Iwaki, Tokyo, Japan) and cultured for 7 days in the following differentiation medium: DMEM/F12 (1:1) supplemented with 10% FBS, without any growth factors [10]. For immunocytochemistry, the cells were fixed in 4% PFA and stained with the following primary antibodies: anti-p75 (rabbit IgG, 1:200, Chemicon) and anti-P0 (PZO; chick IgG, 1:200, Aves Labs), to examine their differentiation into the mature stage of the Schwann-cell lineage. Secondary antibodies were anti-rabbit IgG (Alexa 488) and anti-chick IgG (Alexa 568).

The distal portions of intact or injured sciatic nerves (day 7 after the injury) from MBP-Cre/Floxed-EGFP mice were postfixed for 24 hours in 4% PFA, soaked overnight in 10% sucrose followed by 30% sucrose, and embedded in a cryomold for sectioning at 10 μm. The primary antibodies were anti-GFP (goat IgG, 1:200, Rockland, Gilbertsville, PA) and anti-p75 (rabbit IgG, 1:200, Chemicon). The secondary antibodies were anti-goat IgG (Alexa 488) and anti-rabbit IgG (Alexa 555). Nuclear counterstaining was performed with Hoechst 33342 (10 mg/ml, Sigma). The samples were observed with a confocal laser scanning microscope (LSM510, Carl Zeiss).

To examine the tri-lineage differentiation potential, spheres derived from injured adult sciatic nerves from MBP-Cre/Floxed-CAG-EGFP mice were plated on PLL-coated 8-well chamber slides and cultured for 7 days in the above-described differentiation medium. For immunocytochemistry, the cells were fixed in 4% PFA and stained with the following primary antibodies: anti-GFP (goat IgG, 1:200, Santa Cruz Biotechnology, Santa Cruz, CA, USA), anti-P0 (PZO; chick IgG, 1:200, Aves Labs), anti-S100 (rabbit IgG, 1:500, Dako, Glostrup, Denmark), anti-β-III tubulin (mouse IgG2b, 1:500, Sigma), and anti-αSMA (mouse IgG2a, 1:1000, Sigma). Secondary antibodies were the following: anti-goat IgG (Alexa 488), anti-rabbit IgG (Alexa 555), anti-chick IgG (Alexa 568), anti-mouse IgG2b (Alexa 488), and anti-mouse IgG2a (Alexa 647). The samples were observed with a universal fluorescence microscope (AxioImager M1; Carl Zeiss).

RT-PCR assay. Total RNA was isolated from each sample with Trizol reagent (Invitrogen, Carlsbad, CA, USA) and DNase I treatment. Total RNA (1 μg) was used to synthesize cDNA with oligo-d(T) primers. The cDNA synthesis was performed at 42°C for 50 min in a final volume of 20 μl, according to the manufacturer's instructions for Superscript III reverse transcriptase (Invitrogen). To normalize the template cDNA, the ubiquitously expressed *β-actin* mRNA was used as a reference. PCR was performed with KOD plus DNA polymerase (Toyobo, Osaka, Japan) according to the manufacturer's instructions. The PCR products were resolved by electrophoresis in 1-3% agarose gels, and the bands were visualized with ethidium bromide under UV light [10]. The PCR products were confirmed by sequencing. The primers are listed in Table 1.

Myelination and neurite-extension assays

DRG neurons were co-cultured with cells derived from intact sciatic nerves or Schwann-spheres using the modified method of Hoshikawa et al [13]. The DRGs were taken from adult mice, dissociated with collagenase and trypsin, and seeded on 8-well chamber slides coated with poly-L-lysine at 200,000 cells per well.

Table 1. Primer Sequences.

	Temp.	Size	sense	antisense
Nestin	60	212	CAGCTGAGCCTATAGTTCAACGC	GAAACAAGATCTCAGCAGGCTGAG
Musashi1	60	542	GGCTTCGTCACTTTCATGGACC	GGGAACTGGTAGGTGTAACCAG
Pax3	60	171	AACAAGCTGGAGCCAATCAACTG	CTGAGGTCTGTGGACGGTGCTA
Sox9	60	263	CACGGAACAGACTCACATCTC	TGCTCAGTTCACCGATGTCCA
Sox10	60	134	ACGCACTGAGGACAGCTTTGA	ATGAGGTTATTGACACGGAACTGG
p75	60	115	GAGTGCTGCAAAGCCTGCAA	TGGCGCTCACCACGTCAGAG
β-actin	60	131	TGACAGGATGCAGAAGGAGA	GCTGGAAGGTGGACAGTGAG

doi:10.1371/journal.pone.0021497.t001

Thereafter, 250,000 cells from the spheres or intact nerves were seeded onto the DRG cultures in DMEM/F12 medium. The cocultures were incubated for 2 weeks, and then anti-MBP and anti-βIII-tubulin antibodies were applied, followed by the appropriate secondary antibodies. The proportions of MBP-positive cells (MBP-positive cells/total cells) were counted and the lengths of the longest βIII-tubulin-positive neurite were measured in a 0.6 mm^2 field by surveying six fields. The average was calculated.

Statistical analysis

All values are presented as the mean ± standard error of the mean (SEM). Statistical significance was determined as $p<0.05$ using one-factor ANOVA and the Tukey-Kramer test for the primary and secondary sphere-forming assays. Student's *t*-test was used to compare the data between groups for the myelination and neurite outgrowth assays.

Results

Adult injured sciatic nerves include sphere-forming cells with a high self-renewal capability

To determine whether there were sphere-initiating cells within adult intact and injured peripheral nerves, we cultured cells derived from the intact and injured sciatic nerves of adult *nestin*-EGFP mice [6]. We succeeded in obtaining spheres from the injured sciatic nerves in floating culture, when the nerves were harvested at certain time points after the injury. In contrast, no spheres were obtained from intact sciatic nerves. These spheres from *nestin*-EGFP mice were positive for EGFP, suggesting that they were Nestin-positive immature cells (Fig. 1**A**). The distal part of the sciatic nerves harvested 24 hours to 6 weeks after crush injury, but not at other time points, could successfully generate spheres in floating culture. The sphere-forming capacity peaked in the samples derived from nerves harvested 3 to 10 days after the injury. Quantitative analysis indicated that approximately 1% of all the viable cells were sphere-initiating cells during this time (Fig. 1**B**).

To assess the self-renewing capacity of these spheres, secondary sphere-forming assays were performed. Primary spheres derived from sciatic nerves harvested 7 days after injury were dissociated into single cells and cultured again in the sphere-forming floating medium. As positive controls, the primary spheres of neural crest stem cells obtained from fetal DRG and neural stem cells from fetal striatum were also dissociated and replated to form secondary spheres. Secondary spheres were successfully obtained from the dissociated primary sciatic-nerve-derived spheres, although the sphere-forming rate was lower than the neural crest stem cells and neural stem cells (Fig. 1**C**).

To characterize the sphere-forming cells derived from injured adult sciatic nerves, frozen sections of the spheres were stained with various cell markers. The spheres were positive for both the undifferentiated-cell marker Nestin [14] and the proliferative-cell marker PCNA (Fig. 1**D**). Interestingly, most of the cells in the spheres expressed undifferentiated-Schwann-cell marker, p75, and a small proportion of them were positive for the myelinating-Schwann-cell marker, P0 (Fig. 1**E**). These results suggested that these spheres consisted of Schwann-cell precursors/immature Schwann cells; we therefore called them, "Schwann-spheres."

Characterization of the Schwann-spheres derived from adult injured sciatic nerve

The majority of the cells in the Schwann-spheres were positive for p75, a marker for immature and non-myelinating Schwann cells, whereas very few cells were positive for P0, a marker for myelinating Schwann cells (Fig. 2**A–a and B–a**). We next asked whether the Schwann-spheres could differentiate into mature Schwann cells *in vitro*. After being cultured for 7 days in differentiation medium [10], approximately 37% of the total cells had differentiated into P0-positive mature Schwann cells (Fig. 2**A–b and B–b**), which had a very similar morphology to the mature Schwann cells derived from adult intact sciatic nerves (Fig. 2**A–c and B–c**).

Furthermore, to determine the origin of the Schwann-spheres, we induced a contusive sciatic nerve injury in MBP-Cre/Floxed-EGFP mice. In these transgenic mice, transient activation of the MBP promoter induces Cre-mediated recombination, indelibly tagging the MBP-positive mature Schwann cells with EGFP expression [7,8,9]. Double immunostaining for GFP and p75 in frozen sections of the distal part of the injured sciatic nerves revealed that most of the GFP-positive cells were positive for p75, whereas very few of the GFP-positive cells in intact sciatic nerves were p75-positive (Fig. 3**A**), suggesting that myelinating mature Schwann cells could de-differentiate to the immature stage after peripheral nerve injury. These EGFP-positive cells could form spheres under floating culture conditions (Fig. 3**B**), whereas EGFP-negative cells did not (data not shown). These findings suggested that the spheres were originally derived from MBP-positive mature Schwann cells in the pre-injury sciatic nerves, and that the spheres contained Nestin-positive immature cells (Fig. 1**A**). We also examined the trilineage differentiation potential of the spheres derived from the injured adult sciatic nerves of MBP-Cre/Floxed-EGFP mice. The EGFP+ spheres derived from these injured adult sciatic nerves differentiated into glial cells (Fig. 3**C**), but not into neurons or myofibroblasts (Fig. S1). These spheres could differentiate only into the Schwann-cell lineage, suggesting that mature Schwann cells de-differentiate into Schwann-cell precursors/immature Schwann cells, but not into neural-crest stem cells after injury.

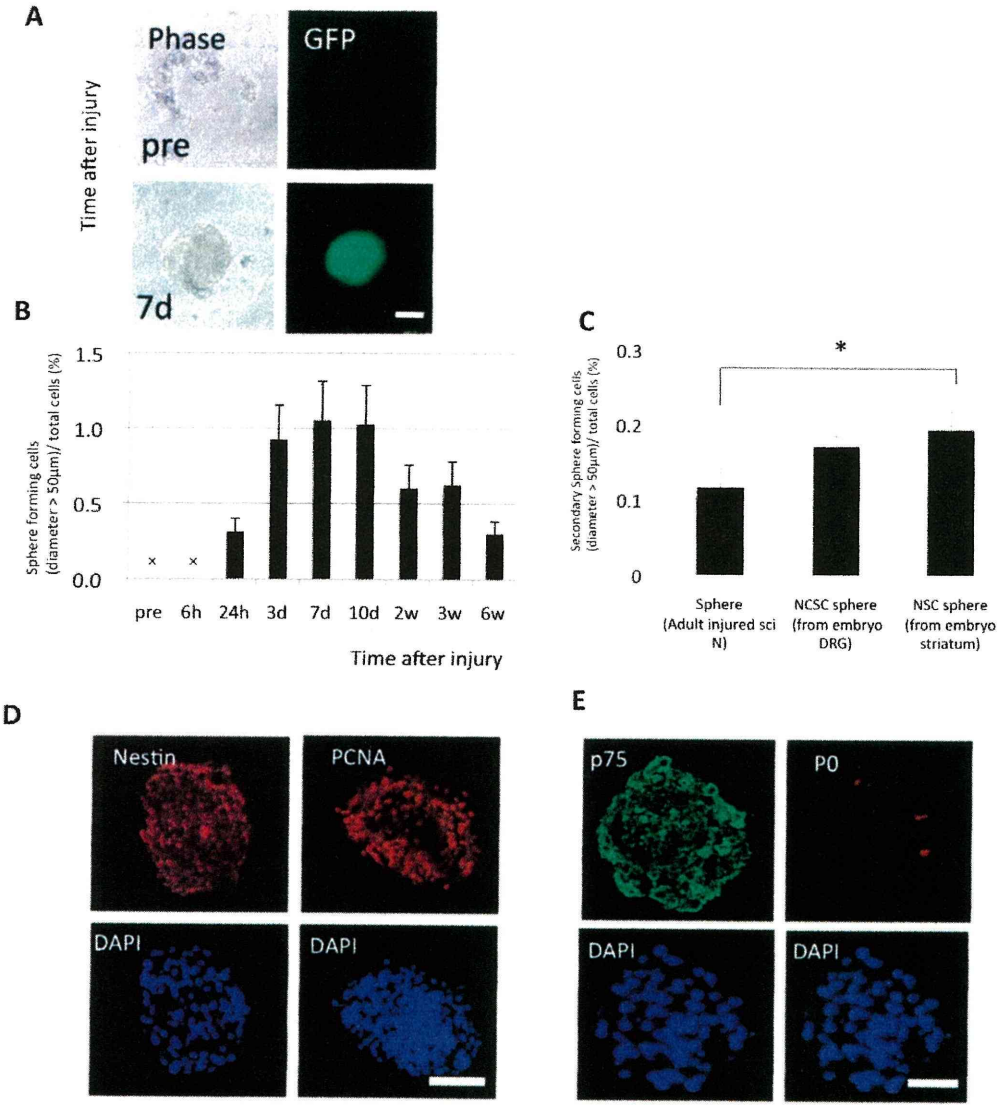

Figure 1. Sphere-forming capacity of cells derived from the injured sciatic nerves of adult mice. (A) Phase-contrast and direct EGFP-fluorescent images showing the spheres formed from the injured nerves of adult *nestin*-EGFP mice were EGFP+ after 7 days in floating culture (pre, pre-injured; 7d, 7 days after injury; Scale bar represents 50 μm). (B) Percentage of sphere-forming cells derived from intact and injured sciatic nerves at 6 or 24 hours, 3, 7, or 10 days, or 2, 3, or 6 weeks after injury (mean ± SEM; n=6 per group; x, no spheres observed). While the sciatic nerves harvested 24 hours to 6 weeks after injury could form spheres under floating culture conditions, those harvested at the other time points did not. (C) Secondary sphere-forming capability of the spheres derived from adult sciatic nerves compared to those derived from neural-crest stem cells (from fetal DRGs) and neural stem cells (from fetal striatum). Spheres from injured adult sciatic nerve could be passaged and formed secondary spheres, indicating their self-renewing ability. One-factor ANOVA and the Tukey-Kramer test were applied (mean ± SEM; n= per group; *$p<0.05$). Scale bar represents 50 μm. (D) The images of immunostained spheres contain Nestin- and PCNA-positive cells. (E) Most of the cells expressed the undifferentiated Schwann cell marker, p75, whereas few cells were positive for myelinating Schwann cell marker, P0. Scale bar represents 50 μm.
doi:10.1371/journal.pone.0021497.g001

Schwann-spheres derived from injured sciatic nerves strongly express immature-Schwann-cell markers

Reverse transcription-polymerase chain reaction (RT-PCR) analysis was conducted to evaluate the mRNA expression of various stem-cell and Schwann-cell markers in the injured adult sciatic nerve-derived spheres and fetal neural crest-derived spheres (Fig. 4). The spheres derived from injured adult sciatic nerves showed higher expression of the immature-neural-precursor cell markers *Nestin* and *Musashi-1* than were seen in the intact and injured adult sciatic nerves. The neural-crest markers *Pax3* and *Sox9* were also expressed in the injured adult sciatic nerves and Schwann-spheres. However, their expression of these genes was lower than that of spheres derived from fetal sciatic nerves or DRGs. Intact and injured adult sciatic nerves, fetal sciatic nerves, DRGs, and striatum all expressed *Sox10* as expected, since this gene is expressed at all stages of the Schwann-cell lineage [15] and is deeply involved in the development of the central nervous system [16]. The expression of *p75*, the marker of immature and non-myelinating Schwann cells, was observed in the adult sciatic-nerve-derived Schwann-spheres, as well in fetal sciatic-nerve- and DRG-derived spheres. Interestingly,

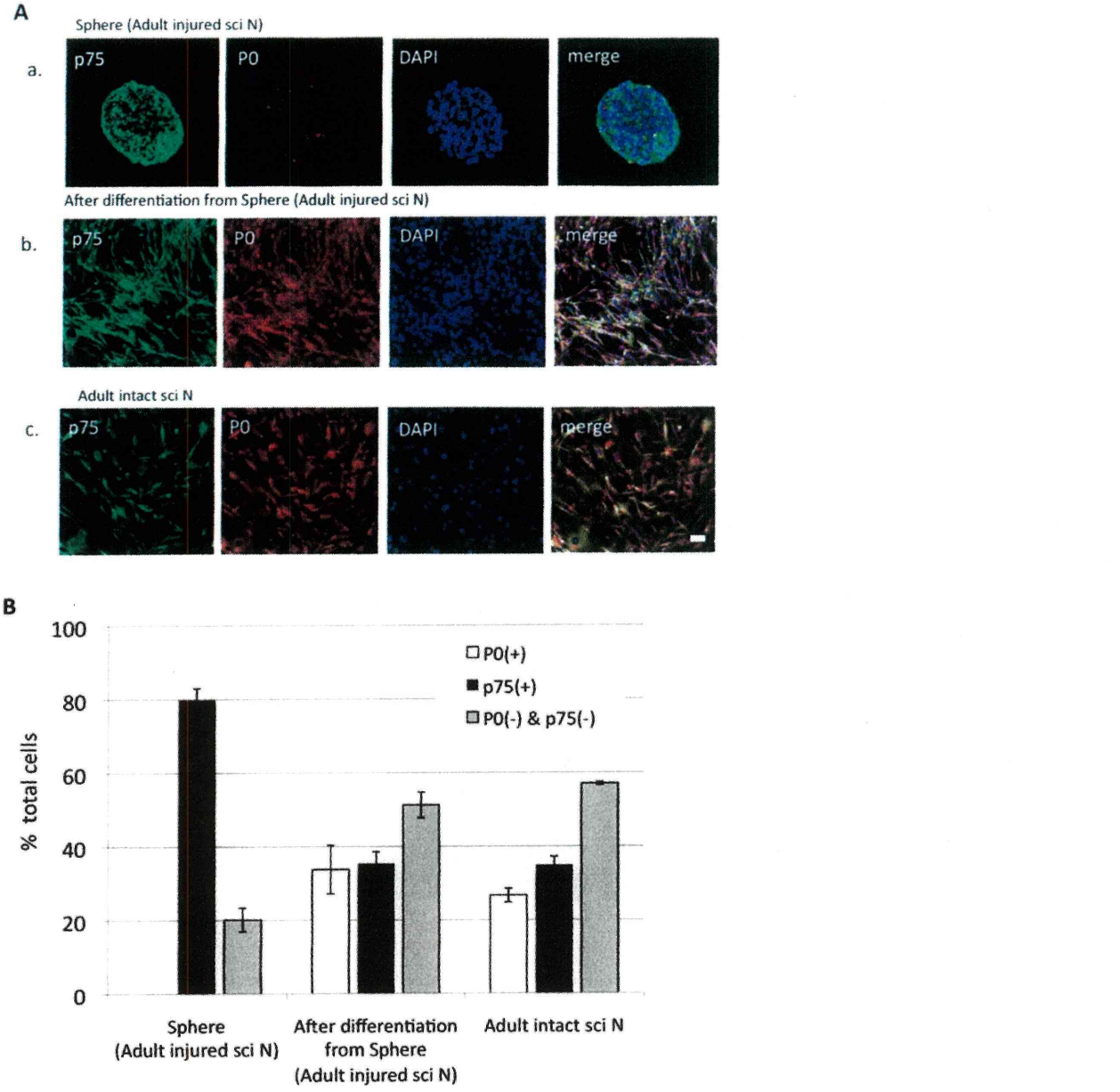

Figure 2. Differentiation assay of the Schwann-spheres derived from injured adult sciatic nerve. Immunostaining (A) with p75, a marker for immature and non-myelinating Schwann cells, and P0, a marker for myelinating Schwann cells, and quantitative analysis (B) (a, Sphere from injured adult sciatic nerves; b, Sphere after differentiation; c, Schwann cells from intact sciatic nerve; mean ± SEM; n = per group). After inducing their differentiation, most Schwann-sphere cells differentiated into P0-positive mature Schwann cells, which closely resembled the Schwann cells from intact sciatic nerves. Scale bar represents 100 μm.
doi:10.1371/journal.pone.0021497.g002

the *p75* expression in the cells from the injured adult sciatic nerve increased after sphere formation, but decreased in the fetal sciatic nerve- and DRG-derived spheres.

Schwann-spheres show higher potentials for myelination and neurite outgrowth than do mature Schwann cells *in vitro*

To examine the Schwann-spheres' therapeutic potential, we performed myelination and neurite growth assays *in vitro* [17]. DRG neurons were co-cultured with mature Schwann cells or with Schwann-spheres derived from injured adult sciatic nerves, and stained for MBP and βIII-tubulin (Fig. 5**A**). Both the number of MBP-positive myelin-forming Schwann cells in myelination assay [13] (Fig. 5**B**) and the length of the βIII-tubulin-positive neuritis in neurite outgrowth assay; [18] (Fig. 5**C**) were significantly greater in the co-culture with the Schwann-spheres derived from injured sciatic nerve compared with the co-culture with mature Schwann cells derived from intact sciatic nerves. Thus, the Schwann-spheres enhanced myelin formation and

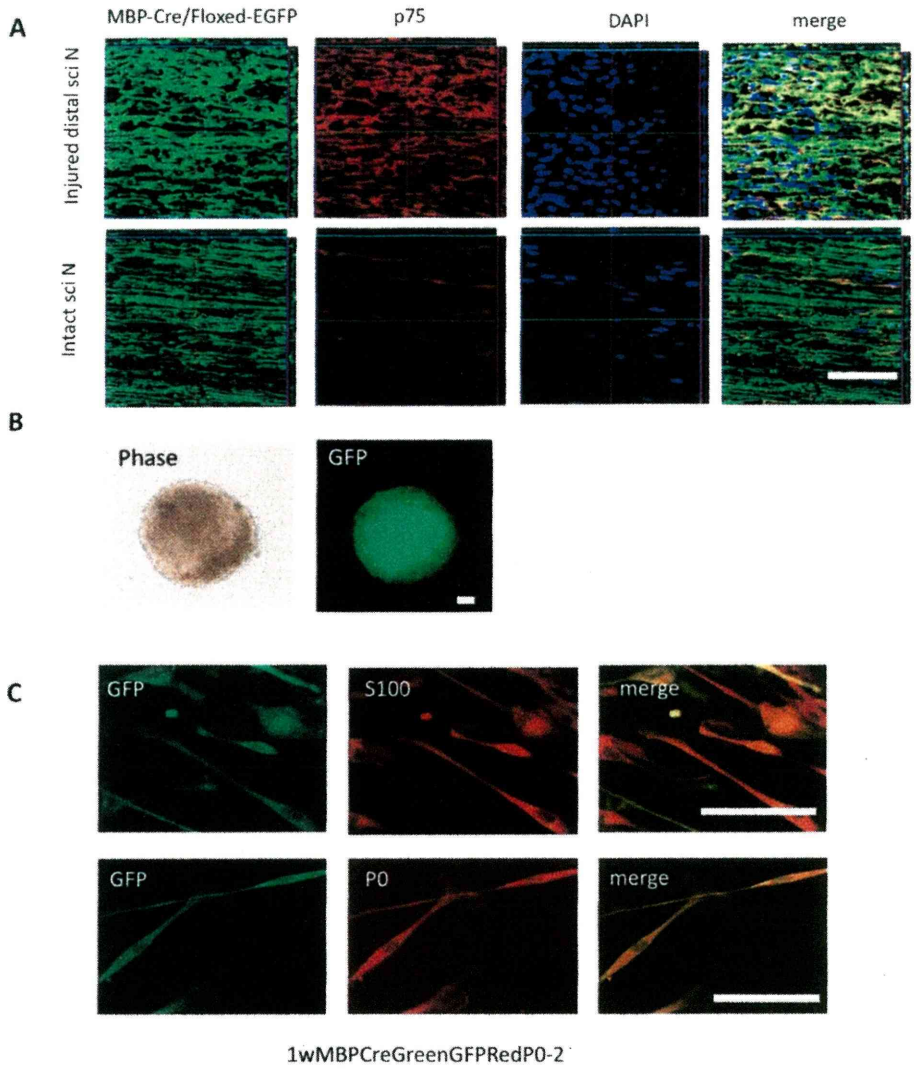

Figure 3. Expression pattern of EGFP in the injured sciatic nerves of adult MBP-Cre/Floxed-EGFP mice. (A) Double immunostaining for GFP and p75 revealed that most of the GFP-positive cells derived from the injured distal sciatic nerves were positive for p75, indicating that the myelinating mature Schwann cells could de-differentiate to an immature stage after peripheral nerve injury. (B) Phase-contrast and direct EGFP-fluorescent images showing that the spheres formed from EGFP+ cells after 7 days in floating culture of the injured peripheral nerves from adult MBP-Cre/Floxed-EGFP mice. (C) Trilineage differentiation potential of the spheres derived from the injured adult sciatic nerves of MBP-Cre/Floxed-EGFP mice. Double immunocytochemistry revealed that the EGFP+ cells were positive for glial-cell markers, S100 and P0. The EGFP+ spheres derived from the injured adult sciatic nerves differentiated into glial cells, but not into neurons or myofibroblasts (Fig. S1). Scale bar represents 50 μm.
doi:10.1371/journal.pone.0021497.g003

neurite outgrowth compared with the effects of mature Schwann cells *in vitro*.

Discussion

This is the first report that Schwann-cell precursors/immature Schwann cells, in the form of cultured "Schwann-spheres," can be isolated from adult peripheral nerves. Mature myelinating and non-myelinating cells respond to nerve injury by reverting to a molecular phenotype similar to that of immature Schwann cells, to provide essential support for axonal regrowth [3]. Therefore, we hypothesized that undifferentiated spheres could be obtained from adult injured peripheral nerves. Indeed, here we demonstrated that adult peripheral nerves harvested at specific time points after contusive injury could generate de-differentiated spheres under the floating culture condition with EGF, FGF and fetal bovine serum (FBS). These Schwann-spheres, which exhibited a high self-renewal capacity, consisted of Schwann-cell precursors/immature Schwann cells. Immunocytochemistry and Cre/lox system-mediated lineage tracing analyses showed that the Schwann-spheres originated from myelinating mature Schwann cells, which de-differentiated after peripheral nerve injury. In addition, immunohistochemical and RT-PCR analyses revealed that the Schwann-spheres could differentiate into the Schwann-cell lineage, suggesting that mature Schwann cells de-differentiate into Schwann-cell precursors/immature Schwann cells, but not into neural-crest stem cells, unlike the spheres derived from fetal sciatic nerves or DRGs.

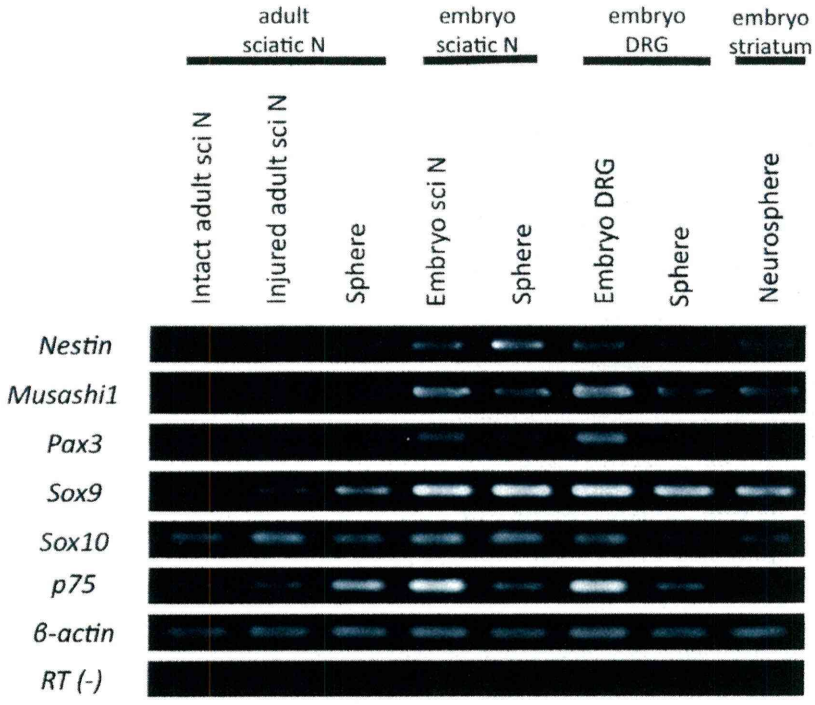

Figure 4. RT-PCR was conducted to evaluate the mRNA expression of various stem-cell and Schwann-cell markers. The injured adult sciatic nerve-derived spheres showed a higher expression of the immature-cell markers *Nestin* and *Musashi-1* and neural-crest markers *Pax3* and *Sox9* than the intact and injured adult sciatic nerves. However, their expression of these genes was lower than that of spheres derived from fetal sciatic nerves and DRGs. The intact and injured adult sciatic nerves, fetal sciatic nerves, DRGs, and striatum expressed *Sox10*. The expression of *p75* was observed in the spheres derived from injured adult sciatic nerves, fetal sciatic nerves, and DRGs.
doi:10.1371/journal.pone.0021497.g004

Schwann cells are considered a promising candidate for cellular transplantation therapies to repair the injured central or peripheral nervous system [19,20,21]. Previous studies have shown that Schwann cells promote axonal growth, mainly from sensory and propriospinal neurons [22]. Moreover, Schwann cells myelinate the ingrowing axons and re-establish axonal conduction [23]. Although Schwann-cell transplants have shown only limited results, in that few long-tract axons enter and few axons exit the grafts [24], a combination therapy of Schwann cells with neuroprotective agents, molecules that modify the glial scar [25,26,27], neurotrophic factors [28,29,30], or camp [31], enhances the ingrowth of long-descending axons and the exit of fibers, thereby improving functional recovery. There is a strong current interest in Schwann-cell-based transplantation strategies for the treatment of spinal cord injuries [17]. However, several steps are needed to isolate and obtain highly enriched populations of mature Schwann cells [32,33]. Moreover, it is difficult to use mature Schwann cells for regenerative medicine because of their low proliferative rate and poor survival when grafted into the injured spinal cord [34,35].

Recently, Agudo et al. reported the novel and potentially useful properties of an early cell in the Schwann-cell lineage, the Schwann-cell precursor [36]. Unlike mature Schwann cells, transplanted Schwann-cell precursors thrive in the spinal cord, where they survive for a long time. However, Schwann-cell precursors/immature Schwann cells have not been identified in adult tissues, and they have not been prospectively isolated from adult animals, although stem/progenitor cells have been detected in and isolated from fetal peripheral nerves [1].

In the present study, we also demonstrated that the Schwann-spheres derived from injured adult sciatic nerves demonstrated much higher potentials for myelin formation and neurite-growth enhancement than mature Schwann cells isolated from intact sciatic nerves *in vitro*. Skin-derived precursor (SKP)-derived Schwann cells can myelinate axons [37] and enhance locomotor recovery better than naive SKPs, when used as a cell-transplantation source after contusion spinal cord injury [36]. Although the Schwann-spheres differentiated only into the Schwann-cell lineage, and not into the trilineages of neurons, glial cells, and myofibroblasts, they provide a more accessible and potential autologous cell source for transplantation to treat the damaged peripheral or central nervous system, such as occurs in spinal cord injury.

Many investigators have studied stem-cell transplantation therapies for regenerating the central nervous system. Although the transplantation of fetal neural stem/progenitor cells into the injured spinal cord can promote functional recovery in adult mice [38], neonatal rats [39], adult rats [40], and common marmosets [41], the use of fetal tissue-derived stem cells still generates some ethical concerns. To regenerate the central nervous system, multipotent somatic stem cells, which were identified in the adult skin [36,42] and bone marrow [10], need to differentiate into glial cells prior to transplantation. In addition, hair follicle stem cells [43,44] promote repair of peripheral nerve injury [45,46] and spinal cord injury [47,48]. However, in the results of experiments using neurospheres derived from pluripotent stem cells (embryonic stem cells and induced pluripotent stem cells), transplantation of the gliogenic secondary neurospheres, but not the neurogenic

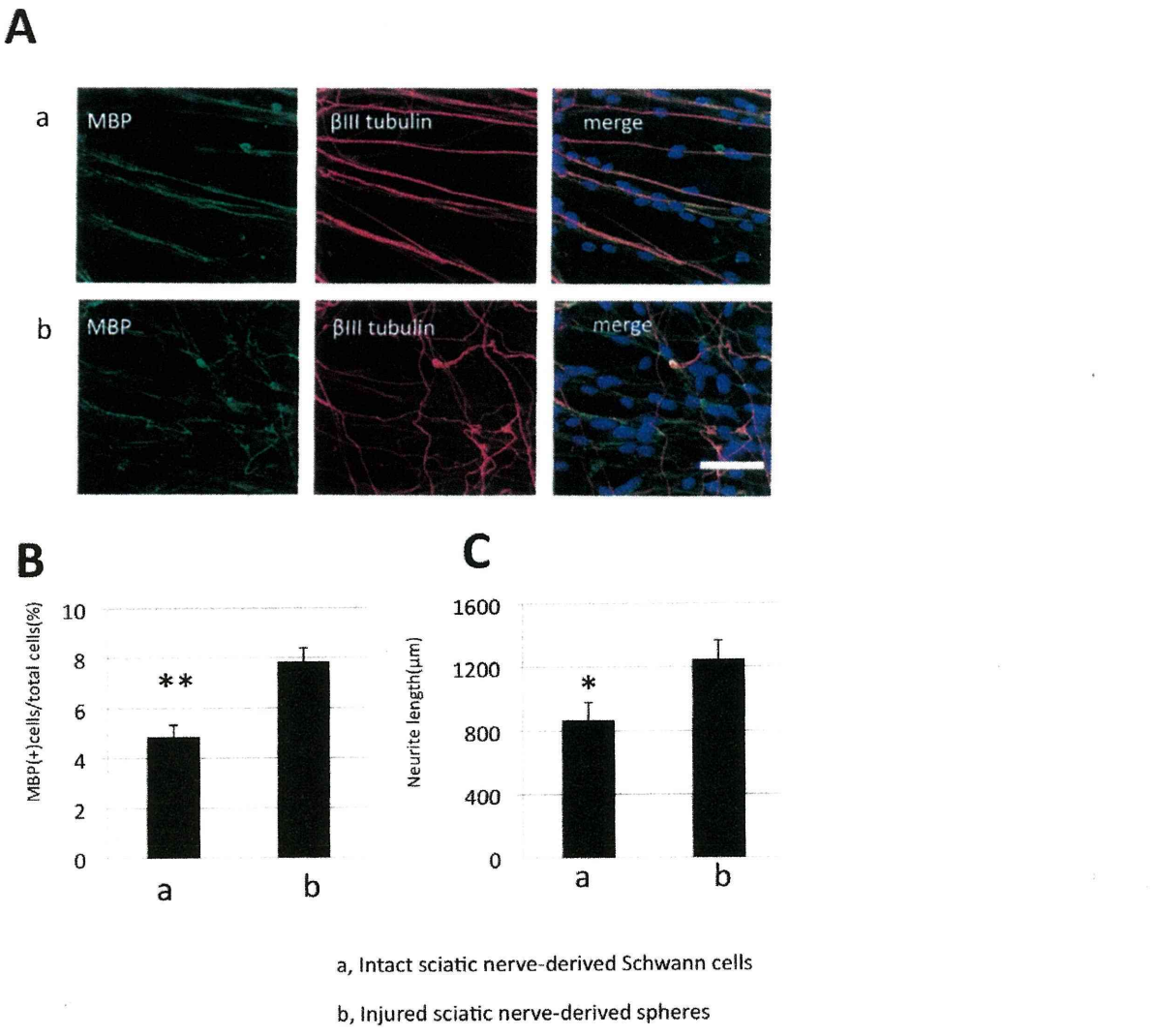

Figure 5. Myelination and neurite-growth assays. DRG neurons were co-cultured with mature Schwann cells from intact sciatic nerves or with Schwann-spheres derived from sciatic nerves harvested 1 week after injury. The cells were then double-stained for MBP and βIII-tubulin (A). The proportion of MBP-positive cells (MBP-positive cells/total cells) (B, myelination assay) and length of the longest βIII-tubulin-positive neurites (C, neurite outgrowth assay) in a 0.6-mm^2 field were measured. Schwann-spheres caused enhanced myelination and neurite outgrowth compared with mature Schwann cells derived from intact sciatic nerves. Student's t-test was used to compare the data between groups (mean ± SEM; n= per group; *, $p<0.05$; **, $p<0.01$). Scale bar represents 50 μm.
doi:10.1371/journal.pone.0021497.g005

primary neurospheres, promoted axonal growth, remyelination, and angiogenesis after spinal cord injury [49,50]. Also in such stem cells, to differentiate into glial cells prior to transplantation might be effective for promoting the recovery from spinal cord injury. Interestingly, Widera et al. very recently reported obtaining spheres from the intact sciatic nerve under serum-free medium [51], while we reported observing sphere formation only from the injured nerve under the medium including serum. The former showed that sphere cells were able to differentiate into ectodermal, mesodermal and endodermal cells, while the latter showed that the spheres were able to differentiate only into glial cells. This discrepancy could be partly because of the differences in the culture conditions. In addition, in agreement with the results of others [4,5], we could not identify nestin-positive cells and spheres in our culture conditions from intact nerves, although we obtained them from injured nerves. Although the spheres that the former reported are more interesting from the biological standpoint, gliogenic spheres such as the spheres in our report might be more effective for the cell transplantation therapies in the same reason. Recently, induced pluripotent stem cells (iPS cells) [52] were recognized as a possible donor source for transplantation therapy, because of their high pluripotency and potential for proliferation. However, a major concern associated with iPS cell-based therapies is tumor formation [53,54], which is correlated with the persistence of undifferentiated cells that remain after differentiation is induced. In contrast, Schwann-spheres, which contain Schwann-cell precursors/immature Schwann cells, but not neural crest stem cells, mostly differentiate into mature Schwann cells without any specific induction protocol. Taken together, our findings indicate that Schwann-spheres could be a novel candidate

for cell-transplantation therapies for the injured central or peripheral nervous system.

Supporting Information

Figure S1 Trilineage differentiation potential of the spheres derived from the injured adult sciatic nerves of MBP-Cre/Floxed-EGFP mice. EGFP+ spheres derived from the injured adult sciatic nerves differentiated into glial cells (Fig. 3**C**), but not into neurons or myofibroblasts. Glial-cell markers, S100, p75, and P0; neuronal markers, NeuN and Hu; myofibroblast marker, SMA. βIII tubulin and peripherin can label peripheral glia in culture, although they are also known as neuronal markers. Scale bar, 50 μm.
(TIF)

References

1. Morrison SJ, White PM, Zock C, Anderson DJ (1999) Prospective identification, isolation by flow cytometry, and in vivo self-renewal of multipotent mammalian neural crest stem cells. Cell 96: 737–749.
2. Mirsky R, Jessen KR, Brennan A, Parkinson D, Dong Z, et al. (2002) Schwann cells as regulators of nerve development. J Physiol Paris 96: 17–24.
3. Jessen KR, Mirsky R (2005) The origin and development of glial cells in peripheral nerves. Nat Rev Neurosci 6: 671–682.
4. Toma JG, Akhavan M, Fernandes KJ, Barnabe-Heider F, Sadikot A, et al. (2001) Isolation of multipotent adult stem cells from the dermis of mammalian skin. Nat Cell Biol 3: 778–784.
5. Wong CE, Paratore C, Dours-Zimmermann MT, Rochat A, Pietri T, et al. (2006) Neural crest-derived cells with stem cell features can be traced back to multiple lineages in the adult skin. J Cell Biol 175: 1005–1015.
6. Kawaguchi A, Miyata T, Sawamoto K, Takashita N, Murayama A, et al. (2001) Nestin-EGFP transgenic mice: visualization of the self-renewal and multipotency of CNS stem cells. Mol Cell Neurosci 17: 259–273.
7. Hisahara S, Araki T, Sugiyama F, Yagami K, Suzuki M, et al. (2000) Targeted expression of baculovirus p35 caspase inhibitor in oligodendrocytes protects mice against autoimmune-mediated demyelination. EMBO J 19: 341–348.
8. Kawamoto S, Niwa H, Tashiro F, Sano S, Kondoh G, et al. (2000) A novel reporter mouse strain that expresses enhanced green fluorescent protein upon Cre-mediated recombination. FEBS Lett 470: 263–268.
9. Kohyama J, Kojima T, Takatsuka E, Yamashita T, Namiki J, et al. (2008) Epigenetic regulation of neural cell differentiation plasticity in the adult mammalian brain. Proc Natl Acad Sci U S A 105: 18012–18017.
10. Nagoshi N, Shibata S, Kubota Y, Nakamura M, Nagai Y, et al. (2008) Ontogeny and multipotency of neural crest-derived stem cells in mouse bone marrow, dorsal root ganglia, and whisker pad. Cell Stem Cell 2: 392–403.
11. Aguayo AJ, David S, Bray GM (1981) Influences of the glial environment on the elongation of axons after injury: transplantation studies in adult rodents. J Exp Biol 95: 231–240.
12. Yoshida S, Shimmura S, Nagoshi N, Fukuda K, Matsuzaki Y, et al. (2006) Isolation of multipotent neural crest-derived stem cells from the adult mouse cornea. Stem Cells 24: 2714–2722.
13. Hoshikawa S, Ogata T, Fujiwara S, Nakamura K, Tanaka S (2008) A novel function of RING finger protein 10 in transcriptional regulation of the myelin-associated glycoprotein gene and myelin formation in Schwann cells. PLoS One 3: e3464.
14. Vukojevic K, Petrovic D, Saraga-Babic M Nestin expression in glial and neuronal progenitors of the developing human spinal ganglia. Gene Expr Patterns 10: 144–151.
15. Kuhlbrodt K, Herbarth B, Sock E, Hermans-Borgmeyer I, Wegner M (1998) Sox10, a novel transcriptional modulator in glial cells. J Neurosci 18: 237–250.
16. Stolt CC, Lommes P, Friedrich RP, Wegner M (2004) Transcription factors Sox8 and Sox10 perform non-equivalent roles during oligodendrocyte development despite functional redundancy. Development 131: 2349–2358.
17. Agudo M, Woodhoo A, Webber D, Mirsky R, Jessen KR, et al. (2008) Schwann cell precursors transplanted into the injured spinal cord multiply, integrate and are permissive for axon growth. Glia 56: 1263–1270.
18. Molteni R, Zheng JQ, Ying Z, Gomez-Pinilla F, Twiss JL (2004) Voluntary exercise increases axonal regeneration from sensory neurons. Proc Natl Acad Sci U S A 101: 8473–8478.
19. Fortun J, Hill CE, Bunge MB (2009) Combinatorial strategies with Schwann cell transplantation to improve repair of the injured spinal cord. Neurosci Lett 456: 124–132.
20. Hood B, Levene HB, Levi AD (2009) Transplantation of autologous Schwann cells for the repair of segmental peripheral nerve defects. Neurosurg Focus 26: E4.
21. Kulbatski I, Mothe AJ, Parr AM, Kim H, Kang CE, et al. (2008) Glial precursor cell transplantation therapy for neurotrauma and multiple sclerosis. Prog Histochem Cytochem 43: 123–176.
22. Xu XM, Zhang SX, Li H, Aebischer P, Bunge MB (1999) Regrowth of axons into the distal spinal cord through a Schwann-cell-seeded mini-channel implanted into hemisected adult rat spinal cord. Eur J Neurosci 11: 1723–1740.
23. Takami T, Oudega M, Bates ML, Wood PM, Kleitman N, et al. (2002) Schwann cell but not olfactory ensheathing glia transplants improve hindlimb locomotor performance in the moderately contused adult rat thoracic spinal cord. J Neurosci 22: 6670–6681.
24. Grimpe B, Pressman Y, Lupa MD, Horn KP, Bunge MB, et al. (2005) The role of proteoglycans in Schwann cell/astrocyte interactions and in regeneration failure at PNS/CNS interfaces. Mol Cell Neurosci 28: 18–29.
25. Plant GW, Bates ML, Bunge MB (2001) Inhibitory proteoglycan immunoreactivity is higher at the caudal than the rostral Schwann cell graft-transected spinal cord interface. Mol Cell Neurosci 17: 471–487.
26. Chau CH, Shum DK, Li H, Pei J, Lui YY, et al. (2004) Chondroitinase ABC enhances axonal regrowth through Schwann cell-seeded guidance channels after spinal cord injury. FASEB J 18: 194–196.
27. Fouad K, Schnell L, Bunge MB, Schwab ME, Liebscher T, et al. (2005) Combining Schwann cell bridges and olfactory-ensheathing glia grafts with chondroitinase promotes locomotor recovery after complete transection of the spinal cord. J Neurosci 25: 1169–1178.
28. Weidner N, Blesch A, Grill RJ, Tuszynski MH (1999) Nerve growth factor-hypersecreting Schwann cell grafts augment and guide spinal cord axonal growth and remyelinate central nervous system axons in a phenotypically appropriate manner that correlates with expression of L1. J Comp Neurol 413: 495–506.
29. Jones LL, Oudega M, Bunge MB, Tuszynski MH (2001) Neurotrophic factors, cellular bridges and gene therapy for spinal cord injury. J Physiol 533: 83–89.
30. Golden KL, Pearse DD, Blits B, Garg MS, Oudega M, et al. (2007) Transduced Schwann cells promote axon growth and myelination after spinal cord injury. Exp Neurol 207: 203–217.
31. Pearse DD, Pereira FC, Marcillo AE, Bates ML, Berrocal YA, et al. (2004) cAMP and Schwann cells promote axonal growth and functional recovery after spinal cord injury. Nat Med 10: 610–616.
32. Casella GT, Bunge RP, Wood PM (1996) Improved method for harvesting human Schwann cells from mature peripheral nerve and expansion in vitro. Glia 17: 327–338.
33. Haastert K, Mauritz C, Chaturvedi S, Grothe C (2007) Human and rat adult Schwann cell cultures: fast and efficient enrichment and highly effective non-viral transfection protocol. Nat Protoc 2: 99–104.
34. Iwashita Y, Fawcett JW, Crang AJ, Franklin RJ, Blakemore WF (2000) Schwann cells transplanted into normal and X-irradiated adult white matter do not migrate extensively and show poor long-term survival. Exp Neurol 164: 292–302.
35. Hill CE, Moon LD, Wood PM, Bunge MB (2006) Labeled Schwann cell transplantation: cell loss, host Schwann cell replacement, and strategies to enhance survival. Glia 53: 338–343.
36. Biernaskie J, Sparling JS, Liu J, Shannon CP, Plemel JR, et al. (2007) Skin-derived precursors generate myelinating Schwann cells that promote remyelination and functional recovery after contusion spinal cord injury. J Neurosci 27: 9545–9559.
37. McKenzie IA, Biernaskie J, Toma JG, Midha R, Miller FD (2006) Skin-derived precursors generate myelinating Schwann cells for the injured and dysmyelinated nervous system. J Neurosci 26: 6651–6660.
38. Cummings BJ, Uchida N, Tamaki SJ, Salazar DL, Hooshmand M, et al. (2005) Human neural stem cells differentiate and promote locomotor recovery in spinal cord-injured mice. Proc Natl Acad Sci U S A 102: 14069–14074.
39. Nakamura M, Okano H, Toyama Y, Dai HN, Finn TP, et al. (2005) Transplantation of embryonic spinal cord-derived neurospheres support growth of supraspinal projections and functional recovery after spinal cord injury in the neonatal rat. J Neurosci Res 81: 457–468.
40. Ogawa Y, Sawamoto K, Miyata T, Miyao S, Watanabe M, et al. (2002) Transplantation of in vitro-expanded fetal neural progenitor cells results in

Acknowledgments

We thank Tokuko Harada for expert animal care, and all the other members of the spinal cord injury research team at Keio University School of Medicine for their enthusiastic discussions, encouragement, and invaluable comments on this study.

Author Contributions

Conceived and designed the experiments: TT KI TY HO MN. Performed the experiments: TT SS AY MS NN HS. Analyzed the data: TT KI MN. Contributed reagents/materials/analysis tools: TT KI SS AY MS NN HS HJO HO MN. Wrote the paper: TT KI SS MN. Supervised the project: YT HO MN.

neurogenesis and functional recovery after spinal cord contusion injury in adult rats. J Neurosci Res 69: 925–933.
41. Iwanami A, Kaneko S, Nakamura M, Kanemura Y, Mori H, et al. (2005) Transplantation of human neural stem cells for spinal cord injury in primates. J Neurosci Res 80: 182–190.
42. Fernandes KJ, McKenzie IA, Mill P, Smith KM, Akhavan M, et al. (2004) A dermal niche for multipotent adult skin-derived precursor cells. Nat Cell Biol 6: 1082–1093.
43. Li L, Mignone J, Yang M, Matic M, Penman S, et al. (2003) Nestin expression in hair follicle sheath progenitor cells. Proc Natl Acad Sci U S A 100: 9958–9961.
44. Amoh Y, Li L, Katsuoka K, Penman S, Hoffman RM (2005) Multipotent nestin-positive, keratin-negative hair-follicle bulge stem cells can form neurons. Proc Natl Acad Sci U S A 102: 5530–5534.
45. Amoh Y, Li L, Campillo R, Kawahara K, Katsuoka K, et al. (2005) Implanted hair follicle stem cells form Schwann cells that support repair of severed peripheral nerves. Proc Natl Acad Sci U S A 102: 17734–17738.
46. Amoh Y, Kanoh M, Niiyama S, Hamada Y, Kawahara K, et al. (2009) Human hair follicle pluripotent stem (hfPS) cells promote regeneration of peripheral-nerve injury: an advantageous alternative to ES and iPS cells. J Cell Biochem 107: 1016–1020.
47. Amoh Y, Li L, Katsuoka K, Hoffman RM (2008) Multipotent hair follicle stem cells promote repair of spinal cord injury and recovery of walking function. Cell Cycle 7: 1865–1869.
48. Liu F, Uchugonova A, Kimura H, Zhang C, Zhao M, et al. (2011) The bulge area is the major hair follicle source of nestin-expressing pluripotent stem cells which can repair the spinal cord compared to the dermal papilla. Cell Cycle 10: 830–839.
49. Kumagai G, Okada Y, Yamane J, Nagoshi N, Kitamura K, et al. (2009) Roles of ES cell-derived gliogenic neural stem/progenitor cells in functional recovery after spinal cord injury. PLoS One 4: e7706.
50. Tsuji O, Miura K, Okada Y, Fujiyoshi K, Mukaino M, et al. (2010) Therapeutic potential of appropriately evaluated safe-induced pluripotent stem cells for spinal cord injury. Proceedings of the National Academy of Sciences of the United States of America 107: 12704–12709.
51. Widera D, Heimann P, Zander C, Imielski Y, Heidbreder M, et al. (2011) Schwann Cells can be reprogrammed to multipotency by culture. Stem Cells Dev. *(in press)*.
52. Takahashi K, Yamanaka S (2006) Induction of pluripotent stem cells from mouse embryonic and adult fibroblast cultures by defined factors. Cell 126: 663–676.
53. Wernig M, Zhao JP, Pruszak J, Hedlund E, Fu D, et al. (2008) Neurons derived from reprogrammed fibroblasts functionally integrate into the fetal brain and improve symptoms of rats with Parkinson's disease. Proc Natl Acad Sci U S A 105: 5856–5861.
54. Miura K, Okada Y, Aoi T, Okada A, Takahashi K, et al. (2009) Variation in the safety of induced pluripotent stem cell lines. Nat Biotechnol 27: 743–745.

Beneficial compaction of spinal cord lesion by migrating astrocytes through glycogen synthase kinase-3 inhibition

*Francois Renault-Mihara[1,2], Hiroyuki Katoh[2,3], Takeshi Ikegami[2,3], Akio Iwanami[2,3], Masahiko Mukaino[2], Akimasa Yasuda[2], Satoshi Nori[2], Yo Mabuchi[1], Hirobumi Tada[1], Shinsuke Shibata[1], Ken Saito[4], Masayuki Matsushita[4], Kozo Kaibuchi[5], Seiji Okada[6], Yoshiaki Toyama[2], Masaya Nakamura[2]**, Hideyuki Okano[1]**

Keywords: astrocyte; glial scar; GSK-3; migration; spinal cord injury

DOI 10.1002/emmm.201100179

Received January 11, 2011
Revised August 11, 2011
Accepted August 31, 2011

The migratory response of astrocytes is essential for restricting inflammation and preserving tissue function after spinal cord injury (SCI), but the mechanisms involved are poorly understood. Here, we observed stimulation of *in vitro* astrocyte migration by the new potent glycogen synthase kinase-3 (GSK-3) inhibitor Ro3303544 and investigated the effect of Ro3303544 administration for 5 days following SCI in mice. This treatment resulted in accelerated migration of reactive astrocytes to sequester inflammatory cells that spared myelinated fibres and significantly promoted functional recovery. Moreover, the decreased extent of chondroitin sulphate proteoglycans and collagen IV demonstrated that scarring was reduced in Ro3303544-treated mice. A variety of *in vitro* and *in vivo* experiments further suggested that GSK-3 inhibition stimulated astrocyte migration by decreasing adhesive activity *via* reduced surface expression of β1-integrin. Our results reveal a novel benefit of GSK-3 inhibition for SCI and suggest that the stimulation of astrocyte migration is a feasible therapeutic strategy for traumatic injury in the central nervous system.

INTRODUCTION

Spinal cord injury (SCI) currently has no satisfying cure. While the therapeutic potential of stem/progenitor cells from various sources, including induced pluripotent stem (iPS) cells (Tsuji et al, 2010), in cell replacement strategies is uncontested (Okano, 2010), numerous obstacles including their potential tumourigenicity (Miura et al, 2009) must be overcome. Alternative, potentially complementary, therapeutic strategies are thus still required.

Recently, using several conditional knock-out mice targeting STAT3 signalling in reactive astrocytes, we and others have observed that the compaction and seclusion of infiltrating inflammatory cells in the lesion centre by migrating reactive astrocytes during the sub-acute phase of SCI is associated with improved locomotor recovery (Herrmann et al, 2008; Okada et al, 2006). These findings suggest that reactive astrocyte migration may constitute a new therapeutic target for the early phase of SCI (Renault-Mihara et al, 2008).

Glycogen synthase kinase-3 (GSK3)-α and β are serine/threonine kinases originally identified as regulators of glycogen synthase. Based on their involvement in several signalling pathways (Forde & Dale, 2007), they are considered potential therapeutic targets for several diseases (Chico et al, 2009). The fibroblast-specific genetic deletion of GSK3-β is associated with

(1) Department of Physiology, Keio University School of Medicine, Tokyo, Japan
(2) Department of Orthopedic Surgery, Keio University School of Medicine, Tokyo, Japan
(3) National Hospital Organization, Murayama Medical Center, Musashi-murayama, Japan
(4) Department of Molecular and Cellular Physiology, Graduate School of Medicine, University of the Ryukyus, Nishihara, Japan
(5) Department of Cell Pharmacology, Graduate School of Medicine, Nagoya University, Nagoya, Japan
(6) Department of Research Superstar Program Stem Cell Unit, Graduate School of Medical Sciences, Kyushu University, Fukuoka, Japan
Corresponding author: Tel: +81 3 5363 3747; Fax: +81 3 3357 5445; E-mail: hidokano@a2.keio.jp
Corresponding author: Tel: +81 3 5363 3812; Fax: +81 3 3353 6597; E-mail: masa@sc.itc.keio.ac.jp

accelerated skin wound closure in mice (Kapoor et al, 2008). Furthermore, GSK-3 inhibition was reported to be beneficial for SCI, possibly by reducing apoptosis and promoting axonal growth (Cuzzocrea et al, 2006; Dill et al, 2008).

Taking advantage of a novel, potent specific inhibitor of GSK-3, Ro3303544, we investigated the effects of GSK-3 inhibition on astrocyte migration capability. The observation that sustained inhibition of GSK-3 stimulated astrocyte migration *in vitro* led us to administer Ro3303544 after contusive SCI in mice and examine the effects of this treatment *in vivo*.

RESULTS

Ro3303544 is more potent than a previously utilized GSK-3 inhibitor

Although the potency and specificity of Ro3303544 have been evaluated in kinase assays (Adachi et al, 2007), its potency was evaluated in more detail in primary cultures of hippocampal neurons, which are recognized as very sensitive to any toxicity. In the absence of Wnt-induced signalling, cytoplasmic β-catenin is constitutively phosphorylated by GSK-3 and degraded by the ubiquitin-proteasome system (Inestrosa & Arenas, 2010). Upon initiation of the Wnt signal and subsequent inhibition of GSK-3 activity, β-catenin accumulates in the cytoplasm, translocates into the nucleus and promotes the transactivation of various genes. Treatment of E17.5 hippocampal neurons with 1 μM Ro3303544 for 48 h resulted in a strong nuclear and peri-nuclear accumulation of β-catenin as expected (Fig 1A).

The potency of Ro3303544 was then compared to another GSK-3 inhibitor, SB415286 (Coghlan et al, 2000), previously used *in vivo* (Dill et al, 2008). To quantify the level of GSK-3 inhibition at various concentrations chosen according to their respective IC50s (0.6 and 78 nM for Ro3303544 and SB415286, respectively), the phosphorylation level of collapsin response mediator protein 2 (CRMP2) at Thr514, a specific site for phosphorylation by GSK-3 (Yoshimura et al, 2005), was examined in hippocampal neurons. Ro3303544 at 500 nM

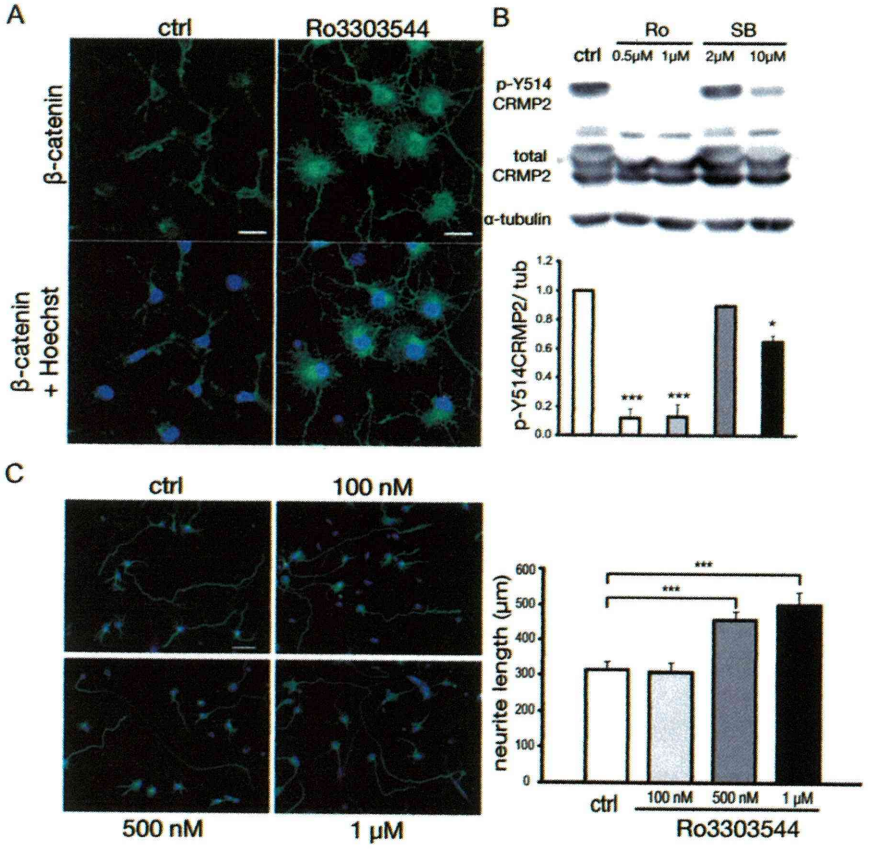

Figure 1. Ro3303544 is more potent than a previously utilized GSK-3 inhibitor.

A. Treatment of E17 rat hippocampal neurons *in vitro* with 1 μM Ro3303544 for 48 h resulted in dramatic nuclear and perinuclear accumulation of β-catenin. Scale bars: 20 μm.

B. Complete abrogation of Thr514-CRMP2 phosphorylation with Ro3303544 under the same conditions as in **A** confirmed the higher potency of Ro33034544 compared to SB415286. Data represent mean ± SEM of three independent experiments. $^{***}p < 0.001$; $^{*}p < 0.05$.

C. Treatment of E17 rat hippocampal neurons *in vitro* with Ro3303544 for 72 h significantly promoted neurite outgrowth. Green: βIII-tubulin, blue: Hoechst. Scale bar: 50 μm. Data represent mean ± SD of three independent experiments performed in triplicate. $^{***}p < 0.001$.

drastically reduced phosphorylation, in contrast to a partial effect of SB415286 at 10 μM (Fig 1B).

The treatment of E17.5 rat hippocampal neurons with Ro3303544 for 72 h *in vitro* resulted in significantly increased neurite length (mean ± SD; 58.83 ± 12.24%; Fig 1C). Together, these experiments demonstrated the high potency of Ro3303544 and its lack of toxicity at the concentrations used.

Sustained inhibition of GSK-3 stimulates the migration of astrocytes *in vitro*

Since the compaction of inflammatory cells in the lesion epicentre by reactive astrocytes during the sub-acute phase of SCI is associated with enhanced locomotor recovery (Herrmann et al, 2008; Okada et al, 2006), the stimulation of astrocyte migration is an attractive approach for the treatment of SCI during the early phase (Renault-Mihara et al, 2008). Considering that activation of the Wnt/β-catenin pathway results in the increased migration of numerous cell types in a variety of pathophysiological contexts, inhibition of GSK-3 leading to activation of β-catenin was speculated to stimulate astrocyte migration. This hypothesis was first tested *in vitro*.

Inhibition of GSK-3 by Ro3303544 was found to compromise the recolonization of a wounded area (Supporting Information, Fig S1A and Supplemental Movie 1), in agreement with the role of GSK-3 in polarization (Etienne-Manneville & Hall, 2003). Sustained GSK-3 inhibition before the migration assay was reasoned to be necessary for activating β-catenin-responsive genes. Treatment for 24 h with Ro3303544 resulted in the nuclear accumulation of β-catenin in astrocytes (Fig 2A) in a dose-dependent manner (Fig S2A and S2B). In agreement with the mitogenic effect of activated β-catenin in various cell types, these doses of Ro3303544 were observed to promote bromodeoxyuridine (BrdU) incorporation in astrocytes *in vitro* (Fig S2C).

Considering that additional treatment time would allow the completion of downstream events, we attempted to extend the Ro3303544 treatment time of astrocytes to 48 h before

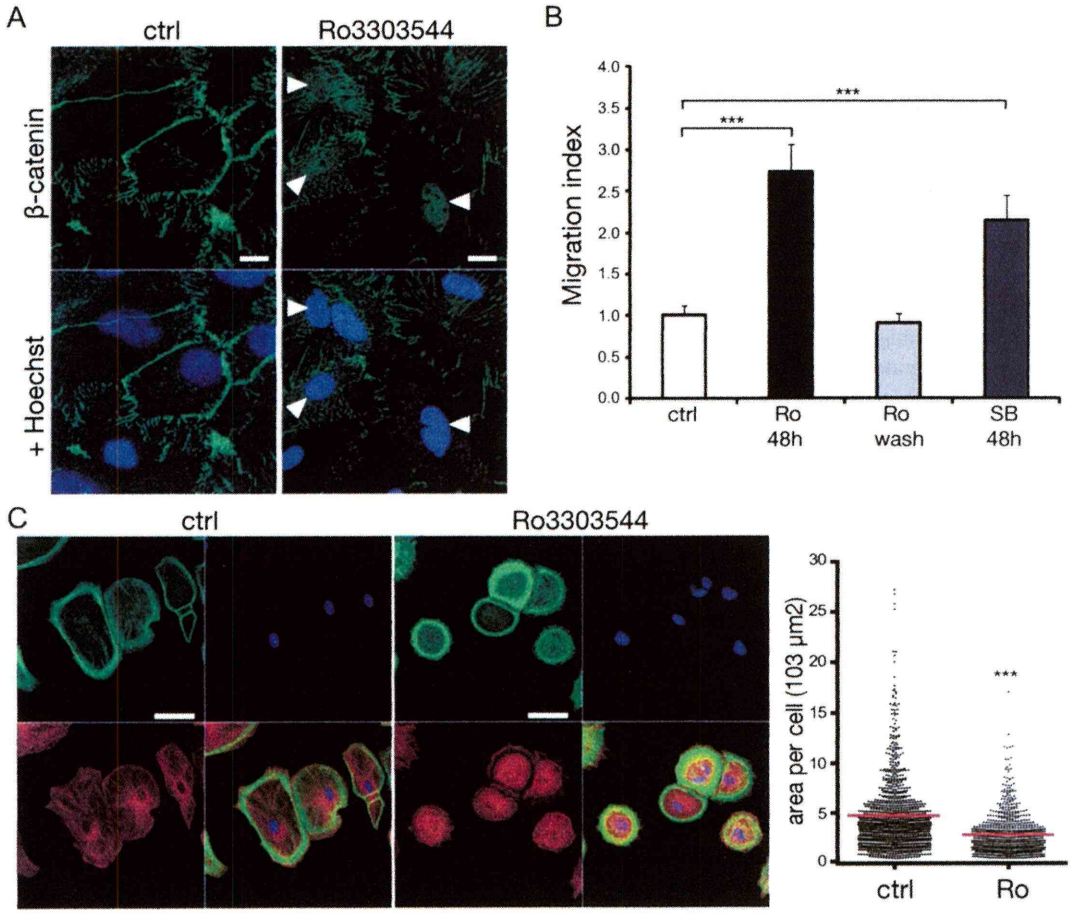

Figure 2. Sustained, but not acute, inhibition of GSK-3 by Ro3303544 stimulates the migration of astrocytes and reduces their spreading *in vitro*.

A. Treatment for 24 h with 1 μM Ro3303544 resulted in the strong nuclear accumulation of β-catenin in astrocytes (white arrowheads). Scale bar: 20 μm.

B. The sustained inhibition of GSK-3 by 48-h pretreatment with either Ro3303544 or SB415286 greatly increased astrocyte migration in a transwell assay. Wash-out of Ro3303544 normalized the migration index. Data represent mean ± SD of three independent experiments. $^{***}p < 0.001$.

C. Pretreatment for 48 h with Ro3303544 before seeding reduced the spreading of astrocytes onto coverslips coated with 10 μg/ml laminin. Green: F-actin labelled with phalloidin; red: α-tubulin; blue: Hoechst nuclear staining. Scale bars: 50 μm.

performing the wound scratch assay in the presence of aphidicolin, a potent antimitotic drug. However, Ro3303544 treatment sustained over 24 h was observed to disrupt the astrocytic monolayer without inducing toxicity (Fig S1B and S1C). Since intercellular contacts, mainly through adherens junctions (Dupin et al, 2009), are required for the effective recolonization of wounded astrocytic monolayers, this monolayer disruption prohibited the evaluation of 'β-catenin-activated' astrocyte migration in this assay. Therefore, a modified Boyden's chamber assay or 'transwell' assay was used, which quantifies the migration of dissociated cells through a porous membrane. Treatment of astrocytes for 48 h with 1 μM Ro3303544 before the transwell assay resulted in a 2.73 ± 0.33-fold increase in cell migration compared to control-treated astrocytes (Fig 2B and Fig S2D). A similar increase observed upon pre-treatment with 10 μM SB415286 (2.15 ± 0.30-fold increase) indicated that the stimulation of astrocyte migration was indeed due to the sustained inhibition of GSK-3, rather than to the effect of Ro3303544. The acute inhibition of GSK-3 by Ro3303544 from 30 min prior to the transwell assay until its end (15 h), a time window similar to that for the wound assay, had no significant effect on cell migration (Fig S2E) indicating that the effect of GSK-3 depended on the cell migration mode.

Dysregulated activation of the Wnt/β-catenin pathway is a common phenomenon in numerous tumours and is associated with metastatic potential (Nguyen et al, 2009). To investigate whether sustained GSK-3 inhibition promoted an irreversible, cancerous transformation of the astrocytes, Ro3303544 was removed after the initial 48 h treatment, and the astrocytes were maintained in control medium for an additional 2 days before testing their migration properties. This wash-out procedure completely normalized the migratory ability of the cells (Fig 2B), suggesting that the pro-migratory effect of sustained Ro3303544 treatment was not related to cancerous cell transformation.

Sustained inhibition of GSK-3 reduces astrocytic spreading *in vitro*

Since alterations in cell migratory properties are often associated with morphological changes, the effects of prolonged Ro3303544 treatment on astrocytic morphology were examined by staining for F-actin and α-tubulin. Ro3303544 or control solution was applied for 48 h, and then the cells were replated at a low density onto laminin-coated coverslips. After 15 h of culture, the astrocytes treated with Ro3303544 remained rounded with intense peripheral actin rings (Fig 2C), in contrast to their control counterparts, which adopted a typical astrocytic morphology. Quantitative morphometric analysis confirmed a significant reduction of the mean area per cell after treatment with Ro3303544 ($4774 \pm 3650\ \mu m^2$ and $2866 \pm 2064\ \mu m^2$, $n = 977$ and 756 analysed cells in the control and Ro3303544 group, respectively), thus demonstrating that sustained inhibition of GSK-3 reduces the spreading of astrocytes.

Inhibition of GSK-3 by Ro3303544 promotes the compaction of infiltrated inflammatory cells after spinal cord injury

Next, the *in vivo* effects of Ro3303544 after SCI were examined. To focus on the compaction of inflammatory cells by reactive astrocytes, the protocol consisted of intraperitoneal administration of Ro3303544 for only the first 5 days after thoracic contusive SCI in mice (Fig 3A). This is in contrast to a previous report in which Dill et al (2008) administered SB415286 for 3–4 weeks after SCI and reported increased axonal growth and improved functional recovery. Axonal growth is a delayed event that commences after the inflammatory reaction has subsided, while the compaction of inflammatory cells by reactive astrocytes occurs during the sub-acute phase of SCI, namely the first 2 weeks after injury in mice (Okada et al, 2006).

First, the efficiency of the protocol was evaluated. Analysis by confocal microscopy revealed that at 4 days post-injury (DPI), while phosphorylated active β-catenin (van Noort et al, 2002) was weakly expressed and localized exclusively to the cytoplasm of neurons in the spinal cords of control mice, administration of Ro3303544 resulted in β-catenin upregulation and nuclear accumulation in neurons and reactive astrocytes (Fig 3C). Immunoblotting of spinal cord lysates collected at 5 DPI quantitatively confirmed this β-catenin activation *in vivo* after administration of Ro3303544 (Fig 3B).

The effect of Ro3303544 on the compaction of inflammatory cells after SCI was then investigated. As previously observed (Okada et al, 2006), CD11b-positive inflammatory cells appeared as a diffuse infiltrate at the lesion centre of the injured spinal cord parenchyma at 7 DPI in both groups (Fig 4A) and were progressively compacted by the surrounding GFAP-positive reactive astrocytes at 14 and 42 DPI. Three-dimensional measurement of the lesion volume through the analysis of GFAP-negative areas in serial sagittal sections revealed that while the initial infiltration of inflammatory cells at 7 DPI was similar in both groups, the compaction of inflammatory cells at 14 DPI was significantly accelerated by Ro3303544 administration, consistent with the *in vitro* stimulation of astrocyte migration by Ro3303544 (Fig 4B). At 14 DPI, confocal microscopic examination of the boundary between reactive astrocytes and the lesion centre visualized through laminin confirmed the potent walling off of the lesion by reactive astrocytes in the Ro3303544-group (Fig 4C).

To examine the possibility that the increased compaction of inflammatory cells upon Ro3303544 administration *in vivo* resulted from enhanced proliferation of reactive astrocytes, BrdU incorporation experiments were performed. Mice in the control and Ro3303544 groups received daily intraperitoneal injections of BrdU for 14 days after the injury. Quantitative analysis revealed no significant difference in the number of BrdU-labelled reactive astrocytes surrounding the lesion, implying that the increased compaction of infiltrated inflammatory cells by Ro3303544 results from the migration of reactive astrocytes rather than from astrocyte proliferation (Fig 4D).

Treatment with Ro3303544 reduces the size of the lesion scar and demyelination

The lesion scar in traumatic SCI consists of a fibrous scar at the lesion core surrounded by a glial scar. Among the numerous molecules that are upregulated in CNS lesions (Sofroniew, 2009), chondroitin sulphate proteoglycans (CSPG) were exam-

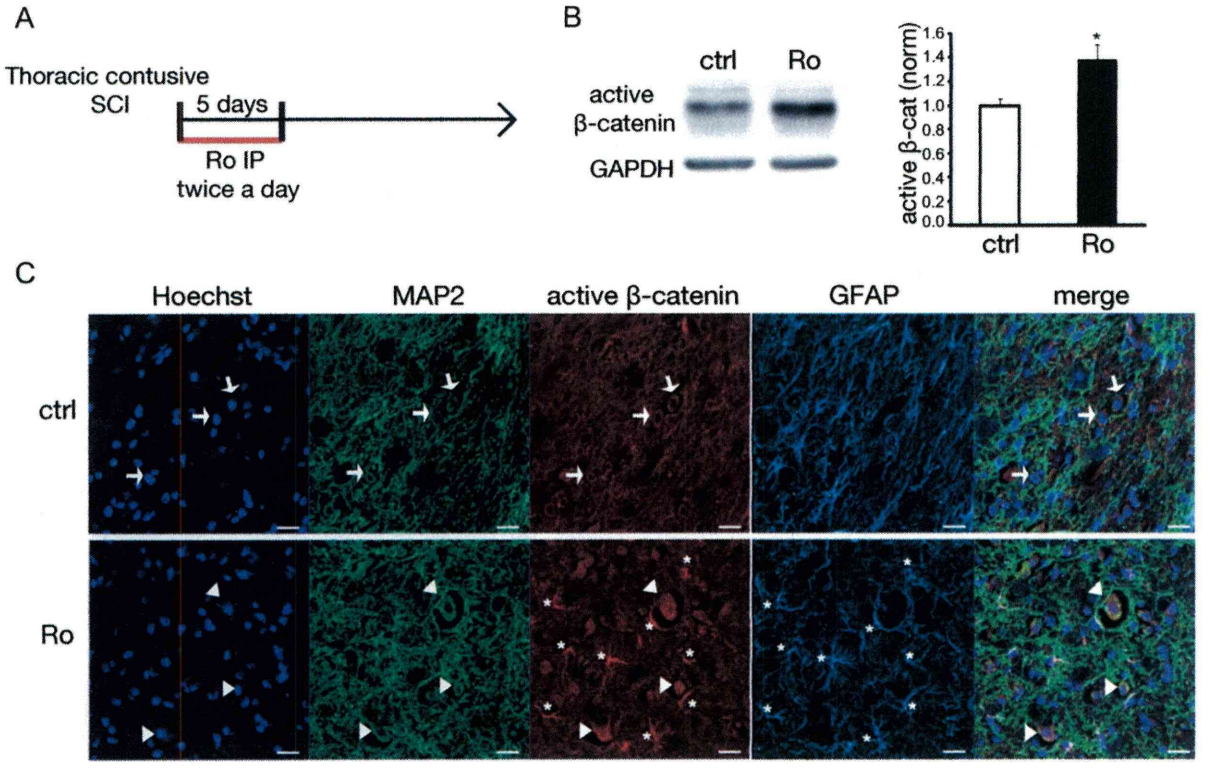

Figure 3. *In vivo* administration of Ro3303544 for the first 5 days after SCI in mice is effective.

A. Experimental design.

B. Immunoblot of spinal cord lysates at 5 DPI revealed that intraperitoneal injections of Ro3303544 potently increased the levels of a phosphorylated active form of β-catenin *in vivo*. Histogram displays the mean ± SEM of one experiment (four mice per group) ($^*p < 0.05$, Wilcoxon rank-sum test).

C. At 4 DPI, confocal analysis showed that while active β-catenin is weakly expressed and localized exclusively to the cytoplasm of neurons in the spinal cords of control mice (arrows), injections of Ro3303544 resulted in drastic upregulation and nuclear accumulation of β-catenin in neurons (arrowheads). Note that the relative upregulation of active β-catenin is even more pronounced in reactive astrocytes (asterisks).

ined first. Seminal studies have shown that CSPG staining overlapped with areas of inflammatory cell infiltration (Fitch & Silver, 1997). Quantitative analysis indicated that the area of CSPG immunoreactivity was significantly reduced in the Ro3303544 group at 14 DPI (Fig 5A) but not at 42 DPI (not shown). Considering that mice harbouring a fibroblast-specific deletion of GSK-3β exhibit accelerated wound closure as well as excessive scarring characterized by elevated collagen production (Kapoor et al, 2008), immunostaining for collagen IV, a major component of the fibrous scar (Klapka & Muller, 2006), was performed. A significant reduction of collagen IV was observed in the Ro3303544 group at 14 DPI (Fig 5B), but again not at 42 DPI (not shown). The reduction of both collagen IV- and CSPG-immunoreactive areas confirms that the stimulation of astrocyte migration by Ro3303544 is associated with reduced scar formation.

An association between compaction of inflammatory cells by migrating reactive astrocytes and a reduction in delayed neuronal damage, such as demyelination, has been previously reported (Herrmann et al, 2008; Okada et al, 2006). Accordingly, while eriochrome cyanine blue staining revealed severe demyelination, as expected, at the lesion level in the control group at 42 DPI, significantly reduced demyelination was observed in the mice treated with Ro3303544 (Fig 6A).

Administration of Ro3303544 improves motor function recovery after spinal cord injury

The recovery of motor function was then monitored over 42 days using the Basso Mouse Scale open-field score (BMS) (Basso et al, 2006). The mice in the Ro3303544 group exhibited a tendency for greater motor function recovery compared to the control group as early as 7 DPI (1.08 ± 0.97 *vs.* 1.85 ± 1.12 in the control and Ro3303544 groups, respectively). Control mice, with a mean BMS score of 2.95 ± 1.21 at 42 DPI, could not support their weight on their hind limbs. By contrast, mice in the Ro3303544 group had a mean BMS score of 5.00 ± 2.05 at 42 DPI, and many mice in this group were able to walk with forelimb–hindlimb coordination. The BMS score of the Ro3303544 group was statistically better than that of the control group (two-way repeated measures ANOVA: *p*-value related to an effect of the treatment = 0.0151), and Bonferroni's multiple comparisons test at each time-point demonstrated statistical significance from 21 DPI until the end of the observation period, *i.e.* 42 DPI (Fig 6B).

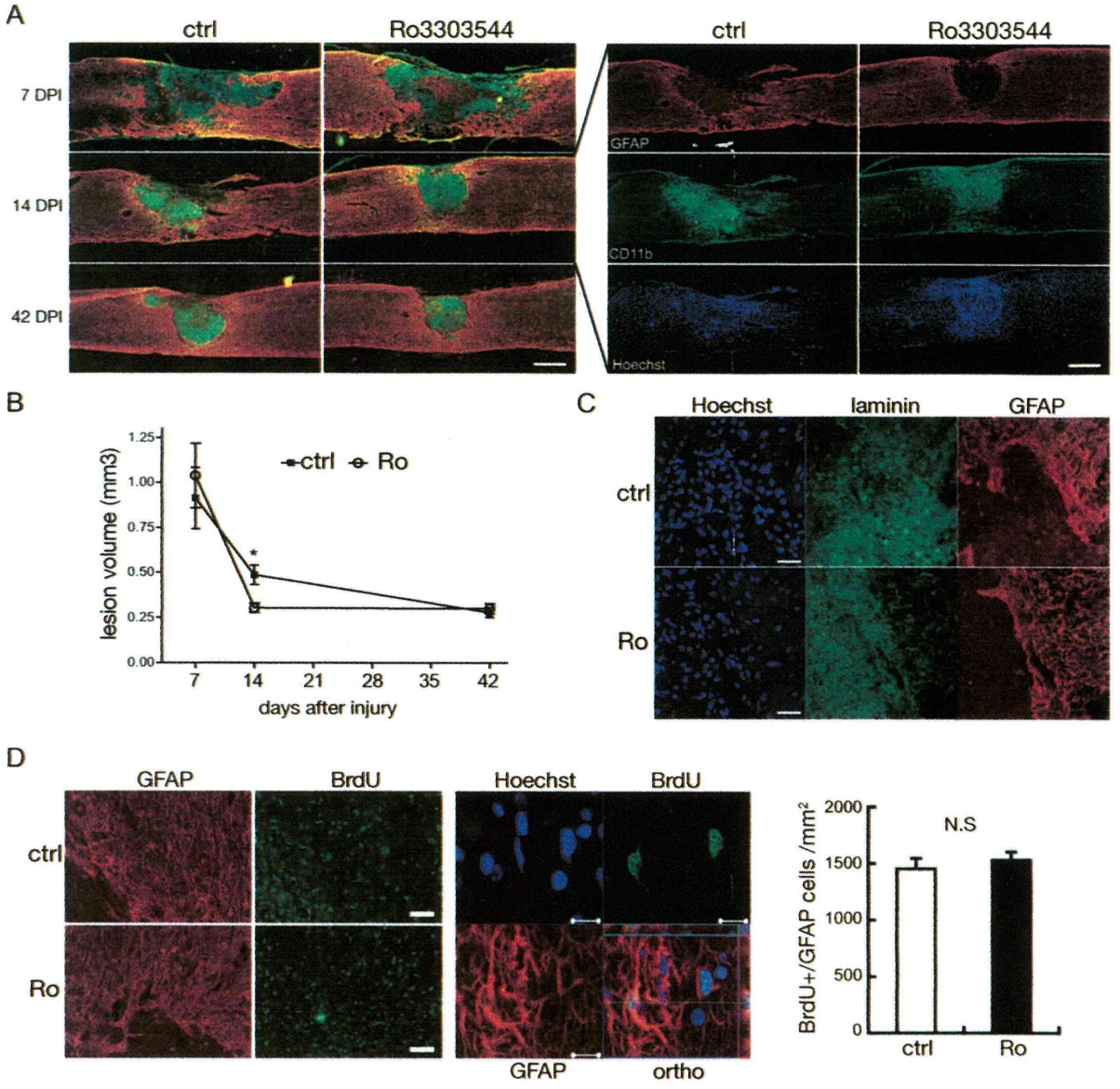

Figure 4. Administration of Ro3303544 after SCI accelerates the compaction of infiltrated inflammatory cells by stimulating reactive astrocyte migration.

A. The compaction of CD11b-positive inflammatory cells surrounded by GFAP-positive reactive astrocytes was significantly accelerated upon Ro3303544 administration. Right panels display the separate immunostaining at 14 DPI. Red: GFAP; green: CD11b; blue: Hoechst nuclear staining. Scale bars: 500 μm.

B. Lesion volume was significantly reduced at 14 DPI in the Ro3303544 group compared to control. Data represent mean ± SEM. $^{*}p = 0.011$ (Mann–Whitney test, $n = 5$ mice per group at 7 DPI and 42 DPI, $n = 12$ and 10 mice at 14 DPI in the control and Ro3303544 groups, respectively.).

C. At 14 DPI, confocal imaging of the boundary between reactive astrocytes and the lesion centre visualized through laminin revealed reactive astrocytes potently walling off the lesion in Ro3303544 group. Scale bar: 50 μm.

D. Quantification of BrdU incorporation during the first 2 weeks after the lesion did not evidence any significant difference between groups, indicating that the increased compaction did not rely on increased astrocyte proliferation *in vivo*. Confocal imaging (middle panel) illustrates BrdU/GFAP positive cells at high magnification. Histogram data represent mean ± SEM. $^{*}p < 0.05$ (Wilcoxon rank-sum test, $n = 5$ and 6 mice in the control and Ro3303544 groups, respectively). Red: GFAP; green: BrdU. Scale bars: 50 and 10 μm in the left and middle panels, respectively.

Stimulation of astrocyte migration by Ro3303544 is mediated by unknown mechanisms

What is the mechanism by which sustained Ro3303544 stimulates the migration of astrocytes? The pro-migratory effect of GSK-3β depletion in fibroblasts relies on the enhanced expression of endothelin-1 (Kapoor et al, 2008). In the case of astrocytes, the concomitant blockade of both endothelin receptors A and B by BQ-123 and BQ-788 (each 1 μM) had no effect on the pro-migratory effect of Ro3303544 (Fig S3A), indicating that different molecular mechanisms

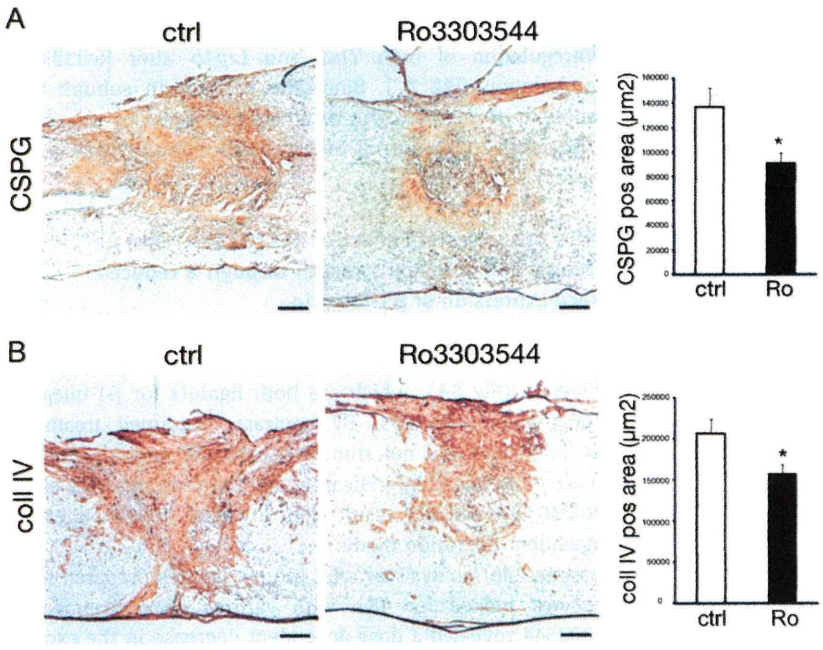

Figure 5. Treatment with Ro3303544 reduces the size of the lesion scar at 14 DPI.

A. The extent of CSPG was significantly reduced at 14 DPI in Ro3303544-treated mice.

B. The fibrous scar, assessed by collagen IV, was also significantly reduced at 14 DPI in Ro3303544-treated mice. In **A** and **B**, data represent mean ± SEM. $^*p < 0.05$ (unpaired *t*-test, $n = 6$ mice per group). Scale bars: 100 µm.

mediate the pro-migratory effect of GSK-3 inactivation/inhibition in astrocytes.

Next, considering that hypoxia-inducible factor 1-α (HIF-1α) promotes cell migration (Le et al, 2004) and that GSK-3 inhibition stabilizes HIF-1α (Flugel et al, 2007), Ro3303544 treatment was investigated to determine whether it could activate HIF signalling. Glioma cells were transfected with reporter constructs in which the expression of firefly luciferase was driven by hypoxia-responsive elements (HRE), and luciferase reporter assays were performed at various time-points during Ro3303544 treatment. While transfection with positive controls, *i.e.* two different gain-of-function HIF-1α mutants, enhanced HIF-dependent luminescence, treatment with Ro3303544 had no effect at any time-point (Fig S3B). This experiment thus ruled out the possible involvement of HIF signalling in the pro-migratory effect of Ro3303544. These results led to the conclusion that the stimulation of astrocyte migration by the sustained inhibition of GSK-3 could involve previously unreported mechanisms.

DNA microarray analysis suggests a global attenuation of integrin signalling in astrocytes by Ro3303544

To gain insight into the molecular mechanism underlying the pro-migratory effect of Ro3303544 treatment, DNA microarray analysis was performed using astrocytes in primary culture treated for 48 h with 1 µM Ro3303544 or control. Considering that wash-out of Ro3303544 normalized astrocyte migration (Fig 2B), this condition was also included as a control for genes that remained highly up- or downregulated after the wash-out period, which would therefore not be relevant to the Ro3303544-enhanced migration.

Figure 7A illustrates the changes in gene expression after treatment with Ro3303544 and demonstrates that the wash-out procedure partially reestablished the normal pattern. Among the 26,734 flags expressed in astrocytes, 1601 and 1638 genes were up- or downregulated more than twofold, respectively, in Ro3303544-treated astrocytes compared to control astrocytes (Fig 7B). In the wash-out *versus* vehicle groups, 1148 and 591 genes were up- or downregulated, respectively, more than twofold. Only 211 genes were upregulated and 573 genes downregulated in both the Ro3303544-treated and wash-out astrocytes compared to the control cells. Of these overlapping genes, all those for which the ratio of intensity (*i.e.* expression level) between the Ro3303544 and washout groups was below twofold were excluded.

To summarize these findings, strong variations were first observed in molecules belonging to the Wnt/β-catenin pathway (Table 1), consistent with the activation of this pathway by the sustained GSK-3 inhibition of Ro3303544. As an example, real-time polymerase chain reaction (qPCR) confirmed the upregulation of *Axin2* (Fig 7C). Considering that the prolonged administration of Ro3303544 drastically affected cell spreading and morphology (Fig 2C), genes related to cell adhesion were then focused on. Integrins are prototypical adhesion receptors that link the extracellular matrix (ECM) to the intracellular actin cytoskeleton. They are heterodimers consisting of an α- and a β-subunit. Within the integrin family, Ro3303544 led to downregulation of the genes for α1, α3, α6, β5, and β1-like integrins, and no member of this family was upregulated (Table 1). Moreover, the expression levels of three genes previously reported to modulate β1-integrin maturation were significantly affected: *N*-acylsphingosine amidohydrolase 3-like (*Asah3l*, also named Acer2; 4.01-fold increase), talin2 (*Tln2*; 52% decrease) and low-density lipoprotein-related protein 1B (*Lrp1b*; 72% decrease).

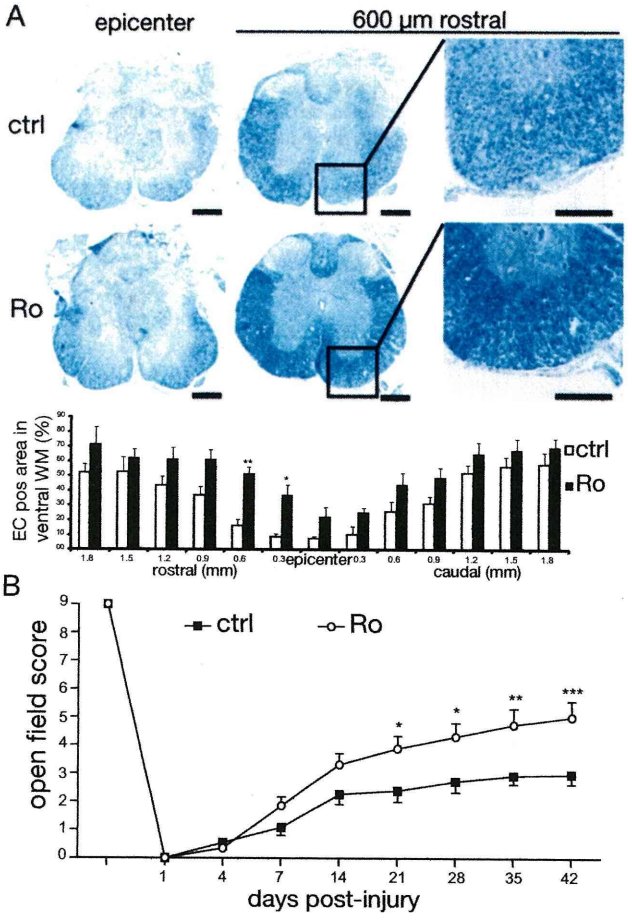

Figure 6. Administration of Ro3303544 reduces demyelination and promotes functional recovery after contusive SCI.

A. Quantitative analysis of eriochrome cyanine-positive areas in the ventral white matter at 42 DPI revealed that treatment with Ro3303544 reduced injury-associated demyelination. Data represent mean ± SEM (**$p < 0.01$, *$p < 0.05$, $n = 5$ mice per group). Scale bars: 250 µm.

B. Hindlimb movement evaluated using the Basso mouse scoring scale improved significantly in the Ro3303544 group compared to the control group from 21 DPI. Data represent mean ± SEM. (*$p < 0.05$, **$p < 0.01$, ***$p < 0.001$; 2-way repeated measures ANOVA followed by Bonferroni *post hoc* test, $n = 12$ and 13 mice in the control and Ro3303544 groups, respectively.)

The β1-integrin subunit is synthesized as an 87-kDa polypeptide that undergoes glycosylations in the endoplasmic reticulum and Golgi apparatus (Akiyama & Yamada, 1987). Only the most glycosylated form of β1-integrin, with a mass of ~130 kDa, is found at the cell surface and functions in cell adhesion or cell signalling, justifying its denomination as the mature form. Importantly, the changes observed in *Asah3l*, *Tln2* and *Lrp1b* suggested that Ro3303544 could cause the reduced maturation of β1-integrin. Asah3l overexpression is indeed known to inhibit β1-integrin maturation and thereby reduce cell adhesion to fibronectin or collagen (Sun et al, 2009). Furthermore, downregulation of *Tln2* and *Lrp1b* is known to reduce β1-integrin maturation and cell adhesion (Albiges-Rizo et al, 1995; Salicioni et al, 2004). qPCR confirmed the downregulation of both *Tln2* and *Lrp1b* after Ro3303544 administration (Fig 7C). Since the β1-integrin subunit is a component of most integrin receptors expressed by astrocytes (Takada et al, 2007), the role of this specific subunit was focused on next.

In vitro pro-migratory effect of Ro3303544 relies on decreased cell adhesion strength through a reduced surface expression of β1-integrin

Ro3303544 induced similar pro-migratory effects in astrocytes seeded on transwell membranes coated with laminin or fibronectin (Fig 8A), which are both ligands for β1-integrin-containing heterodimers. By contrast, sustained treatment with Ro3303544 did not stimulate astrocyte migration in the absence of any coating, indicating that the pro-migratory effect of Ro3303544 did not result from a switch to an adhesion-independent migration mode.

Immunoblot analysis of total protein lysates prepared from astrocytes treated for 48 h with various concentrations of Ro3303544 revealed a dose-dependent decrease in the expression level of the ~130-kDa mature β1-integrin (Fig 8B). The intensity of the ~110-kDa band, corresponding to the precursor form of β1-integrin, was inversely correlated with that of the mature form, suggesting that the process of maturation through glycosylation was indeed inhibited by Ro3303544. Flow cytometry confirmed that the reduction in the ~130-kDa mature form of β1-integrin seen with immunoblotting corresponded to reduced cell-surface expression (Fig 8C). Furthermore, the wash-out procedure partially reversed this reduction of cell-surface β1-integrin, consistent with its involvement in the effect of Ro3303544. Complete abrogation of astrocyte migration by a function-blocking monoclonal antibody against β1-integrin demonstrated that this subunit is necessary for the migration of astrocytes under the conditions in which Ro3303544 exerts its pro-migratory effect (Fig 8D).

In integrin-dependent two-dimensional migration models, the highest migration speeds result from an intermediate level of cell–substratum adhesion strength (net adhesion), which allows both rapid focal contact formation and the generation of traction forces (DiMilla et al, 1991). At low net adhesion, migration rates are indeed impaired because the reduced binding strength lowers the force generated at the leading edge (Gaudet et al, 2003; Palecek et al, 1997). Conversely, high net adhesion slows cells down and favours cell immobilization through delayed rear-process retraction. Three factors define net adhesion: substrate ligand level, integrin expression level, and the integrin–ligand binding affinity.

Reduced expression levels of integrins provide a pro-migratory advantage at high ECM protein concentrations (Palecek et al, 1997). Therefore, the effect of Ro3303544 on migration was examined with increasing concentrations of laminin (Fig 8E). At 2 µg/ml laminin, significantly more control than Ro3303544-treated astrocytes migrated. Although this observation may seem to contradict our initial observation of a Ro3303544 pro-migratory effect at 10 µg/ml ECM coating, it is in good agreement with the model: at above 5 µg/ml laminin,

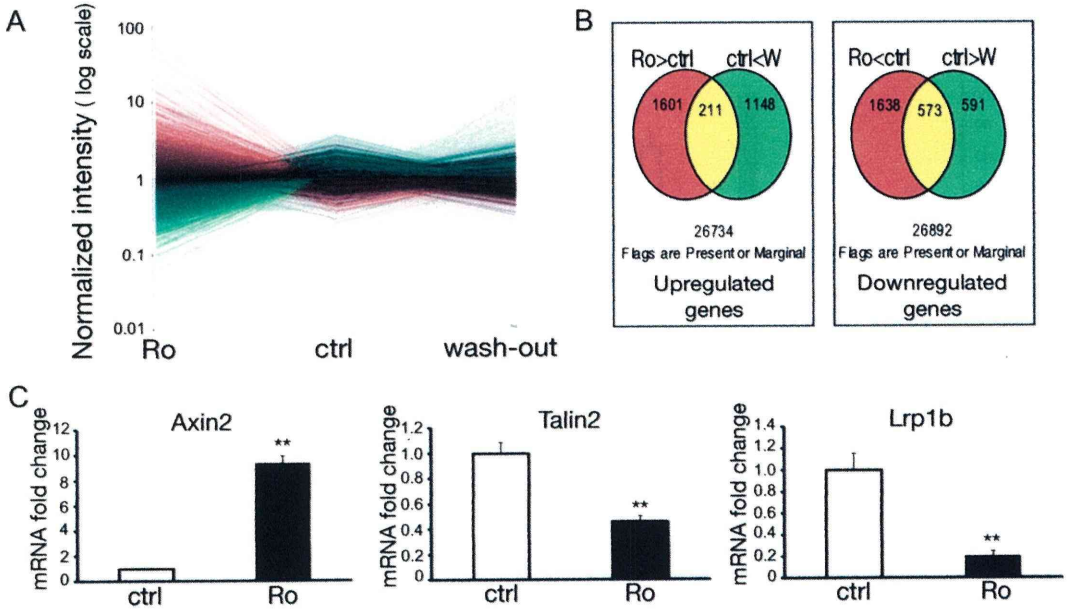

Figure 7. Gene microarray analysis examining the effects of sustained GSK-3 inhibition by Ro3303544 on primary astrocyte cultures.

A. Treatment for 48 h with 1 μM Ro3303544 resulted in a drastic change in the gene expression pattern that could be partially reversed by a 48-h wash-out, $n = 2$ per group. Red: upregulated genes; green: downregulated genes.

B. Diagram illustrating the overlap in genes that were upregulated (left) or downregulated (right) more than twofold in the Ro3303544-treated (Ro: red) and -wash-out (W: green) groups compared to control astrocytes.

C. Significant changes in *Axin2*, *Tln2* and *Lrp1b* mRNA levels detected by qPCR confirmed activation of the Wnt/β-catenin pathway in astrocytes upon prolonged treatment with Ro3303544, as well as the variations in molecules known to modulate β1-integrin signalling. Data represent mean ± SEM. $^{**}p < 0.01$, $n = 5$ (Mann–Whitney test).

treatment with Ro3303544 provided a significant migratory advantage, consistent with the reduced cell-surface expression of β1-integrin in Ro3303544-treated cells. Together, these results suggest that the *in vitro* pro-migratory effect of Ro3303544 relies on decreased adhesion strength, especially through the reduced surface expression of β1-integrin.

Decreased expression of β1-integrin upon Ro3303544 treatment enhances the migration of reactive astrocytes *in vivo*

Since our proposed mechanism for the enhanced migration of astrocytes upon Ro3303544 administration implies the presence of high ECM concentrations, the changes in laminin expression,

Table 1. Gene expression differences of selected gene clusters

Cluster	Abbrev	Accession #	Fold change	Control significance	Ro3303544 significance
Wnt/β-catenin pathway	Apcdd1	AB023957	52.49	P	P
	Wif1	NM_011915	41.02	P	P
	Axin2	NM_015732	20.14	P	P
	Ctnnal1	NM_018761	0.48	P	P
	Wisp2	NM_016873	0.32	P	P
Integrins	Itga3	NM_013565	0.48	P	P
	Itgb5	NM_010580	0.45	P	P
	Itga6	BC024571	0.44	P	P
	Itga6	NM_008397	0.42	P	P
	Itga6	AK045391	0.42	P	P
	Itgbl1	NM_145467	0.42	P	P
	Itga1	AK053377	0.41	P	P
	Itga1	AK053377	0.39	P	P
reported to modulate β1-integrin	Asah3l	NM_139306	4.01	A	P
	Tln2	XM_486227	0.48	P	P
	Lrp1b	BC064765	0.28	P	P, A

P, present; A, absent; ($n = 2$ per group)